國 立 交 通 大 學

電信工程研究所

博 士 論 文

正交分頻多工接取下鏈系統之細胞間干擾抑制技術研究

A Study on Inter-Cell Interference Mitigation Schemes for OFDMA Downlink Systems

研 究 生：邱哲盛

指導教授：黃家齊 博士

中 華 民 國 一百零一 年 七 月

正交分頻多工接取下鏈系統之細胞間干擾抑制技術研究

A Study on Inter-Cell Interference Mitigation Schemes for OFDMA Downlink Systems

研究生：邱哲盛　　Student: Che-Sheng Chiu
指導教授：黃家齊 博士　　Advisor: Dr. Chia-Chi Huang

國立交通大學

電信工程研究所

博士論文

A Dissertation
Submitted to Institute of Communication Engineering
College of Electrical and Computer Engineering
National Chiao Tung University
in Partial Fulfillment of the Requirements
for the Degree of Doctor of Philosophy
in
Communication Engineering
Hsinchu, Taiwan

2012 年 7 月

正交分頻多工接取下鏈系統之細胞間干擾抑制技術研究

研究生：邱哲盛　　指導教授：黃家齊 博士

國立交通大學電信工程研究所

中文摘要

因為能有效提升頻譜使用效率及可提供優異頻率選擇衰落(frequency selective fading)對抗能力，正交分頻多工接取(OFDMA)技術被下一代(4G)行動通信系統廣泛採用，舉凡 LTE/LTE-A 及 Mobile WiMAX/WiMAX 2.0 皆選擇 OFDMA 為下鏈(downlink)傳輸技術。在 OFDMA 下鏈系統中，由於細胞內傳輸具有正交特性因此沒有細胞內干擾(intra-cell interference)，其主要干擾源係來自細胞間干擾(inter-cell interference)，此細胞間干擾問題使得系統效能下降，尤其在細胞邊緣影響更大。然而，考量設計 4G 行動通信系統時，於涵蓋區提供更一致化的用戶體驗(資料速率)是主要發展需求之一，因此細胞間干擾需有效的處理應付。本論文主要探討應用於 OFDMA 下鏈系統之細胞間干擾抑制技術。

細胞間干擾抑制技術主要發展目標為提升細胞邊緣用戶資料速率，而且細胞流通量(throughput)亦要適當維持。近年來，細胞間干擾協調(ICIC)技術被視為是減輕細胞間干擾的有效方法，其中部分頻率重用(PFR)及軟頻率重用(SFR)機制已被下一代行動

通信系統支援實現。本論文第一部份即在探討並比較部分頻率重用及軟頻率重用機制之效能，比較特別的是，此研究係基於 LTE 建議使用之信號強度差額(SSD-based)用戶分群法。我們的研究結果顯示，部分頻率重用及軟頻率重用皆是處理細胞間干擾有效方法，但若考慮用戶資料速率公平性因素，部分頻率重用則可提供較佳之系統容量。

對 3G 行動通信系統而言，軟交遞(soft handover)是用以延伸細胞涵蓋及提升細胞邊緣用戶資料速率的關鍵技術。本論文第二部份提出一創新之混合型細胞間干擾抑制方法，此方法結合部分頻率重用及軟交遞概念，其基本運作原理為利用在部分頻率重用及軟交遞機制之間實行動態選擇(切換)，以提供細胞邊緣用戶更佳之信號品質。根據我們的模擬評估結果顯示，相較於傳統部分頻率重用機制，此混合型細胞間干擾抑制方法的確可大幅改善細胞邊緣流通量，而且在考量用戶資料速率公平性情況下，亦能進一步提升整體細胞流通量。

傳統行動通信網路佈建係以同質網路(homogeneous network)為主，亦即所有節點都是高功率宏基站(macro BS)。然而，為使單位面積系統容量最大化，藉由在宏細胞(macrocell)涵蓋區內佈放多個低功率節點之異質網路(heterogeneous network)或多層次網路佈建方式近來引起極大關注與討論。而且，為增加開放取用(open access)低功率節點卸載宏細胞訊務(traffic)效果，細胞涵蓋擴展(CRE)技術被建議應運用於異質網路佈建。在一個宏細胞搭配特微細胞(picocell)之同頻異質網路佈建(以下簡稱 macro-pico 同頻異質網路)情境下，倘若宏細胞層與特微細胞層之層間干擾無法妥善處理，引入細胞涵蓋擴展技術將可能導致整體網路容量下降。因此，本研究第三部份即提出一種有效之層間干擾協調機制，其適合應用於一個實現細胞涵蓋擴展技術之 macro-pico 同頻異質網路。我們的模擬評估結果說明，此方法確實可顯著改善位於涵蓋擴展區域用戶之信號品質，因而使得系統用戶停運率(outage rate)得以下降；除此，此方法亦能提供相當優異之總體地區流通量增益。

A Study on Inter-Cell Interference Mitigation Schemes for OFDMA Downlink Systems

Student: Che-Sheng Chiu Advisor: Dr. Chia-Chi Huang

Institute of Communication Engineering
National Chiao Tung University

Abstract

Thanks to its effectiveness of improving spectral efficiency and its capability of combating frequency selective fading, orthogonal frequency division multiple access (OFDMA) has been widely adopted in the next generation (i.e. 4th generation (4G)) mobile communication systems as downlink transmission scheme. Considering an OFDMA downlink system, signals originating from the same cell are orthogonal, while those from different cells interfere with each other. As a consequence, inter-cell interference (ICI) becomes a major performance degradation factor, especially on cell borders. Nevertheless, for developing next generation mobile communication systems, a more homogeneous distribution of user data rate over the coverage area is highly desirable. To meet this end, ICI must be effectively managed. In this dissertation, we have studied ICI mitigation schemes in OFDMA systems and especially, we focus on the downlink side.

The objective of ICI mitigation is to provide better service to cell edge users without sacrificing cell throughput. In emerging 4G cellular systems, inter-cell interference

coordination (ICIC) is considered as a promising technique to deal with the ICI. Among the variety of ICIC strategies, the soft frequency reuse (SFR) scheme and the parital frequency reuse (PFR) scheme are widely accepted. In the first part of this research, we review and compare the throughput performance of PFR and SFR in a multi-cell OFDMA downlink system and especially, this work is done by using the signal strength difference based (SSD-based) user grouping method, which is recommended by Long Term Evolution (LTE) standard. We show that both PFR and SFR are very effective ways to cope with ICI in an OFDMA downlink system, but PFR is a more appropriate one to achieve data-rate fairness among users with having an acceptable system capacity.

It is well-known that soft handover is a key technique to extend the cell coverage and to increase the cell edge user data rate in 3G cellular communication systems. In the second part of this research, we deliver a hybrid ICI mitigation scheme which combines PFR and soft handover. Its basic principle is to dynamically choose between a partial frequency reuse scheme (with a reuse factor of 3) and a soft handover scheme to provide better signal quality for cell edge users. Simulation results show that this hybrid scheme yields a significant cell edge throughput gain over the standard PFR scheme. Furthermore, considering data rate fairness among users, the proposed hybrid method also outperforms the standard PFR scheme in total cell throughput.

Traditionally, mobile cellular networks are typically deployed as homogeneous networks in which only high-power macro base stations are contained. Recently, heterogeneous networks (HetNets) or multi-layered network, in which low-power nodes (LPNs) are deployed within macrocell layout, has attracted a lot of interest as a way to maximize system capacity per unit area. Moreover, in order to extent the coverage region of open access LPNs and hence offload more traffics from macrocells, cell range expansion (CRE) strategy is suggested to apply in HetNets. However, assuming a co-channel macro-pico HetNet, the total network throughput could actually decrease due to CRE if the

inter-layer interference couldn’t be effectively managed. The third part of this research presents an inter-layer interference coordination (ILIC) scheme for an OFDMA co-channel macro-pico HetNet that carries out CRE technique. Our simulation results confirm that the proposed ILIC scheme can lead to a significant improvement in link quality for those users in the extended region and thus reduce user outage rate in the system; and further, it can provide a substantial total area throughput gain over the conventional reuse-1 scheme.

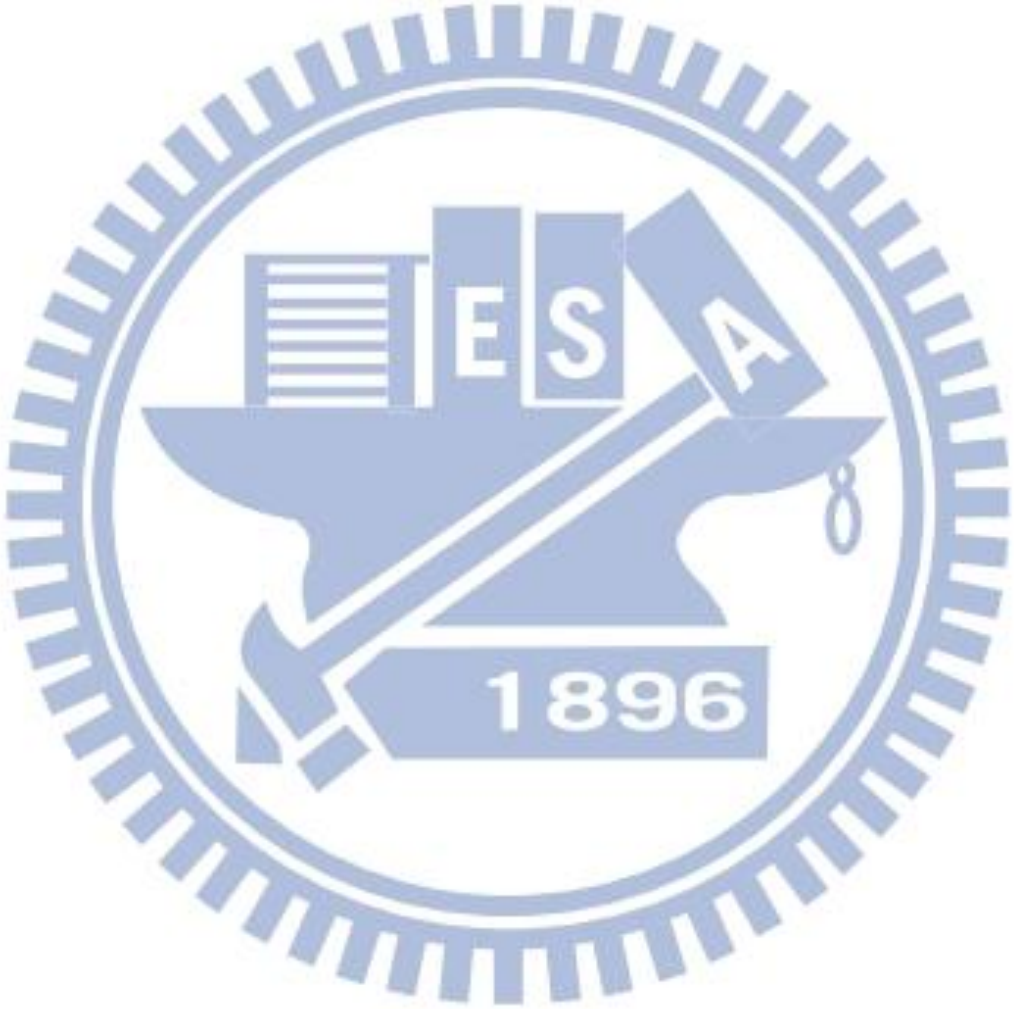

誌　謝

本論文得以順利完成，有賴生命中許許多多貴人的指導、協助、包容與相伴，於此，以感恩之心，謹將此論文獻給您們！

首先，我要以最誠摯的敬意感謝我的指導老師 黃家齊教授，承蒙老師自碩士至博士多年來的指導，讓我在行動通信系統的專業知識領域多有成長，並能在相關研究上有所突破，老師嚴謹認真的治學精神與謙沖的待人處事態度更是學生的典範。

另外，也要感謝本論文的口試委員吳文榕教授、林大衛教授、李程輝教授、陳逸萍技術長、黃正光教授及古孟霖教授，能在百忙當中撥冗費心審查，對論文內容提出懇切的意見與指導，讓本論文能更臻完善。

於此，也要特別感謝中華電信陳榮義協理及研究院楊文豪所長的提攜與推薦，讓我有機會完成博士學位的進修。計畫主管陳瓊璋博士與同事在工作上給予的包容與協助，我更是銘感於心，每位同事的專業素養，也讓我在通訊知識上能不斷成長。

最後，我要將此喜悅與我最親愛的家人分享。父母親自小全心全意的照顧與教誨，讓我能以樂觀進取之心平順克服學業與職場的挑戰，而我親愛的老婆杏玉、女兒亭涵及兒子子鳴，更是我精神上最大的支柱，有你們陪伴的每一天，生活中總是歡樂喜悅與滿滿的幸福，我愛你們也謝謝你們。

Contents

List of Tables

List of Figures

Abbreviations

3D：three dimensions

3G：third generation

3GPP：3rd Generation Partnership Project

4G：fourth generation

ABS：almost blank subframe

AMC：adaptive modulation and coding

BS：base station

CAGR：compound annual growth rate

CDF：cumulative distributed function

CDMA：code division multiple access

CEU：cell edge user

CIU：cell interior user

CoMP：coordinated multi-point

CRE：cell range expansion

CSG：closed subscriber group

EV-DO：Evolution-Data Optimized

HetNet：heterogeneous network

HSPA：High Speed Packet Access

ICI：inter-cell interference

ICIC：inter-cell interference coordination

IEEE：Institute of Electrical and Electronics Engineers

ILI：inter-layer interference

ILIC：inter-layer interference coordination

ISD：inter-site distance

ITU：International Telecommunications Union

ITU-R：The ITU Radiocommunication Sector

JT：joint transmission

LPN：low-power node

LTE：Long Term Evolution

LTE-A：LTE-Advanced

NB：normal band

OFDM：orthogonal frequency division multiplexing

OFDMA：orthogonal frequency division multiple access

OSG：open subscriber group

PB：platinum band

PFR：partial frequency reuse/partial reuse

RAN：radio access network

RSS：received signal strength

SE：spectral efficiency

SFR：soft frequency reuse

SH：soft handover

SINR：signal to interference plus noise power ratio

SNR：signal to noise ratio

SSD：signal strength difference

TDM：time-division multiplexing

UE：user equipment

UMTS：Universal Mobile Telecommunication System

WCDMA：Wideband Code Division Multiple Access

WiMAX：Worldwide Interoperability for Microwave Access

WiMAX 2.0：WiMAX Release 2

Chapter 1 Introduction

1.1 Toward IMT-Advanced/4G

Mobile broadband traffic has surpassed voice and is continuing to grow at an unprecedented rate. This traffic growth, driven by new services and sophisticated devices, is paralleled by user expectations for data rates similar to those of fixed broadband. Cisco predicted that mobile data traffic will grow at a CAGR (compound annual growth rate) of 78% from 2011 to 2016 and increase 18-fold between 2011 and 2016 (see Fig. 1-1) [1]. Accordingly, mobile broadband networks need to handle the predicted data traffic volumes and meet ever-increasing consumer data rate demands in a responsive manner.

3G technologies, such as UMTS/WCDMA/HSPA and cdma2000/EV-DO, are now widely deployed around the world. Because it became clear that 3G systems would be unable to cost-effectively meet with the exploding demand for mobile broadband services, work on post-3G mobile standards was begun a number of years ago. In the recent years, the post-3G standards that have the greatest attractions are 3GPP LTE and Mobile WiMAX

(based on the IEEE 802.16e [2]).

IMT-Advanced (IMT-A) is a next-generation mobile communication technology defined by ITU that includes capabilities exceeding those of IMT-2000 (3G) mobile communication. ITU refers to IMT-A as a 4G mobile communication technology. Note that IMT-A specification is call for 100 Mbps downloads and a 1Gbps link for stationary or local area connections [3]. Although both LTE and Mobile WiMAX are commonly referred to as 4G, but they are not really "*official*" 4G standards, since neither strictly meets all of the requirements set by the IMT-A for 4G technology. To satisfy the IMT-A requirements, LTE performance is upgraded with LTE-Advanced (LTE-A) (i.e. LTE Release 10 and beyond) [15], while Mobile WiMAX is upgraded to WiMAX 2.0 (based on the IEEE 802.16m [4]). In the beginning of 2012, the ITU-R approved both 3GPP LTE-A and WiMAX 2.0 as IMT-A/4G standards.

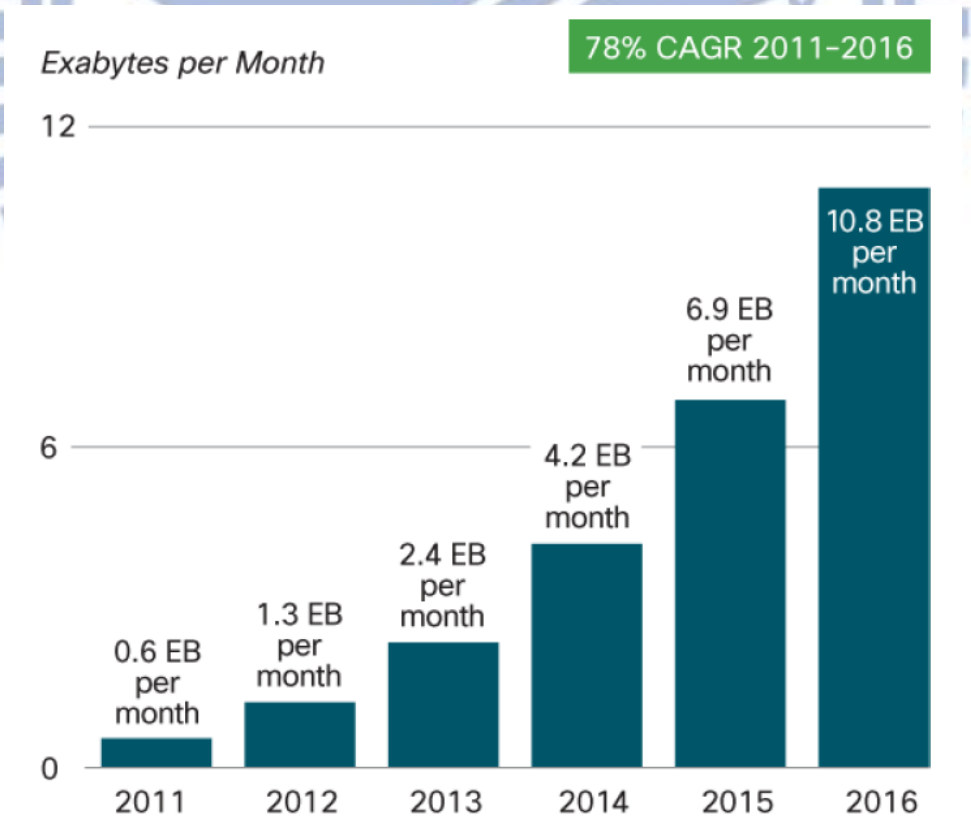

Fig. 1-1 Global mobile data traffic forecast (source: Cisco VNI [1])

The LTE and Mobile WiMAX systems will deliver a much higher bit rate as well as offer the best potential to address the mobile data capacity needs. At the present time, LTE has become the global cellular technology platform of choice for both UMTS/WCDMA/HSPA and cdma2000/EV-DO operators. And further, most of major Mobile WiMAX operators are planned to switch to TD-LTE. Obviously, LTE is expected to dominate next generation (4G) mobile market.

1.2 Problem and Motivation

Orthogonal frequency division multiplexing (OFDM) is a transmission technique that has been widely accepted as a suitable solution for broadband wireless communications due to its efficient frequency domain processing and inherent ability to tolerate severe delay spreads. As an extension, OFDM could be used not only as a modulation scheme, but also as part of the multiple access technique as well, namely orthogonal frequency division multiple access (OFDMA). In OFDMA, the subcarriers are efficiently grouped into many frequency *subchannels* and each user is assigned a fraction of all available subchannels. Accordingly, OFDMA provides a natural and flexible multiple access method.

Recently, OFDMA is considered a most promising multiple access technique to improve spectral efficiency in future mobile communication systems. Two emerging 4G standards, 3GPP LTE and Mobile WiMAX, both exclusively choose OFDMA as the downlink transmission scheme [4, 5]. With orthogonality within the cell, the main interference in an OFDMA system comes from *inter-cell interference* (ICI). The ICI is particularly disadvantageous to user equipments (UEs) located at cell edge, especially for a multi-cell OFDMA system with universal frequency reuse.

In order to maximize spectral efficiency, the emerging OFDMA systems (including LTE and Mobile WiMAX) assume that a frequency reuse factor of 1 (reuse-1) should be

used, i.e., the same frequency band can be used in any cell (sector) of the system. Although full frequency reuse may ensure the good throughput, it brings low signal quality for cell edge users due to ICI. Note that for 3G CDMA systems, a frequency reuse factor of 1 is normally used because CDMA takes advantage of processing gain achieved through using nearly orthogonal spreading codes.

Important criteria for system evaluation and performance requirements are given in a 3GPP technical report [6]. This document lists different requirement items among which we highlight the particular one which says, "Increase cell edge bit rate whilst maintaining same site locations as deployed today". This criterion indicates that the cell edge quality of service (QoS) is an important performance requirement. More specifically, for developing next generation (i.e. 4G) mobile communication systems, a more homogeneous distribution of user data rate over the coverage area is highly desirable [7, 8]. To meet this end, a special focus should be put on improving the cell edge performance and therefore, ICI must be effectively managed.

To deal with this interference problem, 3GPP LTE and Mobile WiMAX both employ inter-cell interference coordination (ICIC) as an interference mitigation scheme. The common theme of ICIC is to apply restrictions to the usage of downlink/uplink resources e.g., time/frequency resources and/or transmit power resources. Such coordination will provide a way to avoid severe ICI, and thus provide more balanced bit rates among UEs. Note that in an LTE network the coordination messages for ICIC can be exchanged over the X2 interface between base stations (BSs). Several ICIC schemes have been proposed for OFDMA systems, including partial frequency reuse (also known as fractional frequency reuse) [9, 10], soft frequency reuse [11, 12], inverted frequency reuse [13], etc.. Among the variety of ICIC strategies, partial frequency reuse (PFR) and soft frequency reuse (SFR) were suggested as the two most promising approaches for ICI mitigation and

have been supported in the nowadays OFDMA systems, in which the representative one is 3GPP LTE [14]. Accordingly, the performances and the relative comparisons of the two ICIC schemes are worthy to study. To this end, one goal of this dissertation is to investigate the throughput performance of PFR and SFR schemes based on the signal strength difference based (SSD-based) user classification method in an OFDMA downlink system. Not that the SSD-based user grouping method is recommended by 3GPP LTE for ICIC operations; and further, to what we know, there is no other study presenting the performance comparisons under the SSD-based method so far.

Most recently, coordinated multi-point (CoMP) transmission and reception is being extensively discussed within the context of 3GPP LTE-A (specified in LTE Release 11 and beyond) [15, 16]. The basic idea behind CoMP is to apply *tight* coordination between the transmissions at different cell sites, thereby achieving higher system capacity and, especially important, improved *cell-edge* data rates. In 3GPP LTE-A, the studied downlink CoMP techniques are coordinated scheduling and coordinated beamforming (CS/CB), joint transmission (JT), and dynamic cell selection (DCS). We refer the readers to [16, 17] for a comprehensive overview of CoMP technology developments.

The coherent combining used in CoMP JT is somewhat like soft handover, a technique that is widely known in CDMA systems in which the same signal is transmitted from different cells [18]. Moreover, to some extent, ICIC can be seen as another simple CoMP transmission scheme which relies on resource management cooperation among base stations [19]. For an OFDMA downlink system, considering a cell edge UE, it could be beneficial if the transmissions can be dynamically switched between a coherent CoMP JT scheme and an ICIC scheme. Hence, in this dissertation, we will deliver an effective hybrid ICI mitigation scheme that resorts to both soft handover and partial frequency reuse. Note that macro diversity technology for soft handover in CDMA mobile communication

systems can be considered as the earliest application of CoMP joint transmission technology in actual communication system. Then we prove that the proposed approach is a good choice to enhance cell edge data rate and overall system capacity.

A conventional cellular network containing *only* high-power macro base stations (macrocells) is termed as a homogeneous network. Recently, the concept of heterogeneous networks (also called HetNets) has attracted a lot of interest and has been brought into 3GPP LTE-A (LTE Release 10) as an efficient way to provide addition capacity needs (per unit area) [15][20]. A HetNet refers to a network deployment in which a large number of low-power nodes (LPNs) or small cells are placed throughout a macrocell layout. In other words, HetNet deployments consist of overlapping cell layers with large differences in the cell output power. To overlay on top of the traditional macrocells, three different types of LPNs have been considered in 3GPP LTE-A for HetNet deployments, including picocells, femtocells, as well as relay stations [15][21]. Picocells are typically outdoor open-access nodes deployed by operators; femtocells normally utilize the closed subscriber group (CSG) feature and are user-deployed; relay stations are nodes which do not have a wired backhaul connection and in general utilize the same spectrum as the donor base station to convey backhaul transmissions (self-backhauling) [15]. These overlaid LPNs offload the macrocells, and more importantly, they provide a significant capacity gain via higher *spatial spectrum reuse*. Moreover, they can be used to enhance the receptions in poor coverage areas. In this dissertation, we will focus on a HetNet deployment consisting of macrocells with embedded picocells and it will be referred to as macro-pico HetNet. Note that among the LPNs in a HetNet, picocells are gained the most attention of 3GPP [22].

The most basic means to operate a HetNet is to apply complete frequency separation between different layers, i.e. operate different layers on different non-overlapping carrier frequencies and thereby avoid any interference between layers. However, due to limited

spectrum resources, the simultaneous use of the same spectrum in different cell layers is highly desirable. Therefore, a co-channel macro-pico HetNet is assumed.

In order to expand the downlink coverage of picocells in the presence of a macrocell and thus to further gain the offloading advantages, the concept of cell range expansion (CRE) [23, 24] has been recently introduced. Although CRE may increase downlink footprints of picocells, it also results in severe inter-layer interference in picocell expanded regions, because the users in the range extension area are not connected to the cells that provide the strongest downlink power. Therefore, range expansion needs to be supported by inter-layer interference coordination (ILIC) between macrocells and overlaid picocells.

Due to the difference in transmission powers of macrocells and picocells, interference-layer interference (ILI) in a co-channel macro-pico HetNet becomes a challenging issue and could be more difficult to handle than in a traditional homogeneous (macro-only) network, especially when CRE technique is carried out. To this end, 3GPP LTE-A mainly includes a TDM solution and in this approach transmissions from macrocells causing high interference onto picocell users are periodically muted during entire subframes (called almost blank subframes (ABSs)) [21][25]. However, this time domain ILIC scheme requires tightly time synchronization between macro and pico layers and could be difficult to always guarantee in the practice. As a consequence, simpler frequency domain and/or power domain ILIC methods are then worthy to study. In this dissertation, considering an OFDMA downlink system, we deliver an ILIC scheme for a co-channel macro-pico HetNet that makes use of frequency domain and power domain coordination. We then confirm that the proposed ILIC method is very useful for enhancing the system performances in a co-channel macro-pico HetNet with picocell range expansion technique.

1.3 Organization of the Dissertation

The rest of this dissertation is organized as follows. In Chapter 2, considering an OFDMA downlink system, the performances of partial frequency reuse and soft frequency reuse have been evaluated and compared based on the signal strength difference based user classification method, which is adopted in the LTE standard. We show that both partial frequency reuse and soft frequency reuse schemes are very effective ways to ameliorate cell edge performance. Besides, we demonstrate that partial frequency reuse yields better throughput as compared with the soft frequency reuse under a well-defined data-rate fairness criterion. In Chapter 3, we propose a hybrid inter-cell interference mitigation scheme for an OFDMA downlink system, which makes use of both partial frequency reuse and soft handover. The basic idea of this hybrid scheme is to dynamically select between a partial frequency reuse scheme and a soft handover scheme to provide better signal quality for cell edge users. We then confirm that the proposed scheme is a competitive choice to further improve cell edge bit rate and overall system capacity. Chapter 4 presents an inter-layer interference coordination scheme on the downlink side for an OFDMA co-channel macro-pico HetNet that carries out CRE technique. The idea of the proposed method is to coordinate frequency and power resources among macrocells and picocells with a set of resource allocation rules. The numerical evaluation and system simulation results demonstrate the applicability and effectiveness of the proposed ILIC scheme. Chapter 5 draws some conclusions.

Chapter 2 On the Performance of Inter-Cell Interference Coordination Schemes in Cellular Homogeneous Networks

2.1 Introduction

Recently, research activities outlined two most promising ICIC schemes for the next generation OFDMA downlink systems: one is partial frequency reuse (PFR) (also known as fractional frequency reuse) [9, 10] and the other one is soft frequency reuse (SFR) [11, 12]. It is worthy to note that both PFR and SFR schemes are adopted in 3GPP LTE, while only PFR is supported in Mobile WiMAX.

In order to carry out ICIC schemes, there is a need to classify users into cell interior

users and cell edge users. A commonly used approach is to distinguish UEs based on the geometry factor or the *G-factor*, which is the average wideband signal to interference plus noise power ratio (SINR) measured by user equipment (UE), compared with a predefined threshold [26-30]. This is a most straightforward approach since a cell edge user always faces noticeable SINR degradation. However, under the consensus that the same measure used for handover reporting should be used for the identification of interior/edge users, the signal strength difference based (SSD-based) method was suggested in 3GPP LTE as a more feasible alternative for ICIC operations [31, 32].

In an OFDMA downlink system, the performance comparisons of PFR and SFR schemes have been conducted by simulations and analyses in [29] and [33-35]. However, there is not a comprehensive study of comparison between these two schemes. Furthermore, to our knowledge, the comparisons between PFR and SFR schemes under SSD-based user classification method have not been covered in the literature yet. It should be noted that different user classification method may lead to different simulation results.

In this chapter, we investigate the throughput performance of PFR and SFR schemes in an OFDMA downlink system based on the SSD-based user classification method, and furthermore, by using a well defined data-rate fairness index, we compare the performance between PFR and SFR schemes with each other. The remainder of this chapter is organized as follows. In Section 2.2, we describe the PFR and SFR schemes. In Section 2.3, we illustrate the SSD-based user grouping method for ICIC applications. In Section 2.4, the method of cell capacity analysis is discussed. In Section 2.5, we first explain the simulation methodologies, and then provide the numerical results and discussions. Finally, concluding remarks are drawn in Section 2.6.

2.2 Inter-Cell Interference Coordination Schemes

We consider a conventional tri-sector cellular system. Throughout this chapter, we assume that each cell[1] always uses its maximum total transmission power, which is kept as a constant. Note that the assumption of full power transmission is reasonable since the transmissions for high speed data traffic in HSPA (High Speed Packet Access) and LTE are generally performed at full power [36].

2.2.1 Partial Frequency Reuse

Partial frequency reuse (PFR) or simply partial reuse (PR) is an ICIC scheme that applies restrictions to the frequency resources in a coordinated way among cells. The idea of PFR is to partition the whole frequency band into two parts, F_1 and F_3, where F_3 is further divided into three subsets; and thus, it results in four orthogonal subbands, F_1, F_{3A}, F_{3B} and F_{3C} (see Fig. 2-1). Note that it is reasonable to assume that F_{3A}, F_{3B} and F_{3C} have the same bandwidth. The frequency subband F_1 is called the cell center band, for which a frequency reuse factor of 1 (reuse-1) is adopted, and it is used by the cell interior users only. On the other hand, the frequency subband F_3 is called the cell edge band, for which a frequency reuse factor of 3 (reuse-3) is implemented, and the cell edge users are restricted to use this frequency subband only. Nevertheless, when the cell edge band is not occupied by the cell edge users, it can also be used by the cell interior users. Note that in a tri-sector network, a frequency reuse factor of 3 means that a frequency subchannel can only be reused in one of the three sectors of the same site.

[1] Normally, the geographical areas that controlled by the same (macro) base station (or Node B) are known as sectors. However, the terms cell and sector are interchangeable in this research.

In [37], an effective reuse factor (ERF) γ_{eff} is introduced to represent the ratio of the total spectrum to the spectrum that can be used in each cell, and it is expressed by

$$r_{eff} = BW_{all} / BW_{cell} = \frac{BW_{F_1} + BW_{F_3}}{BW_{F_1} + (1/3) \cdot BW_{F_3}} \text{ (>1 in PFR)}, \tag{2-1}$$

where BW_{all} denotes the whole bandwidth; BW_{cell} denotes the available bandwidth in each cell; BW_{F_1} and BW_{F_3} denote the bandwidth of reuse-1 and reuse-3 subbands, respectively. Note that the whole bandwidth is the sum of bandwidth BW_{F_1} and BW_{F_3}, and each cell can use the entire BW_{F_1} and 1/3 of BW_{F_3}, i.e., $BW_{F_{3A}}$, $BW_{F_{3B}}$ or $BW_{F_{3C}}$. The effective reuse factor of this scheme is always greater than one. From (2-1), one can calculate the bandwidth of reuse-1 and reuse-3 as follows:

$$BW_{F_1} = BW_{all} \cdot \frac{3 - r_{eff}}{2 \cdot r_{eff}}, \tag{2-2}$$

$$BW_{F_3} = BW_{all} \cdot \frac{3 \cdot r_{eff} - 3}{2 \cdot r_{eff}}. \tag{2-3}$$

Figure 2-1 shows the spectrum setting for partial frequency reuse in a tri-sector cellular layout. We assume that transmit power is equally spread over the whole available bandwidth in each cell, i.e., a flat transmission power spectrum density is assumed (see Fig. 2-1). As we have the constant total power assumption, the transmit power level α can be increased in partial frequency reuse scheme as compared with the pure reuse-1 scheme (i.e. $\alpha > P_1$ in Fig. 2-1) and in this case, the power amplification factor α / P_1 would be the same as the effective reuse factor γ_{eff}.

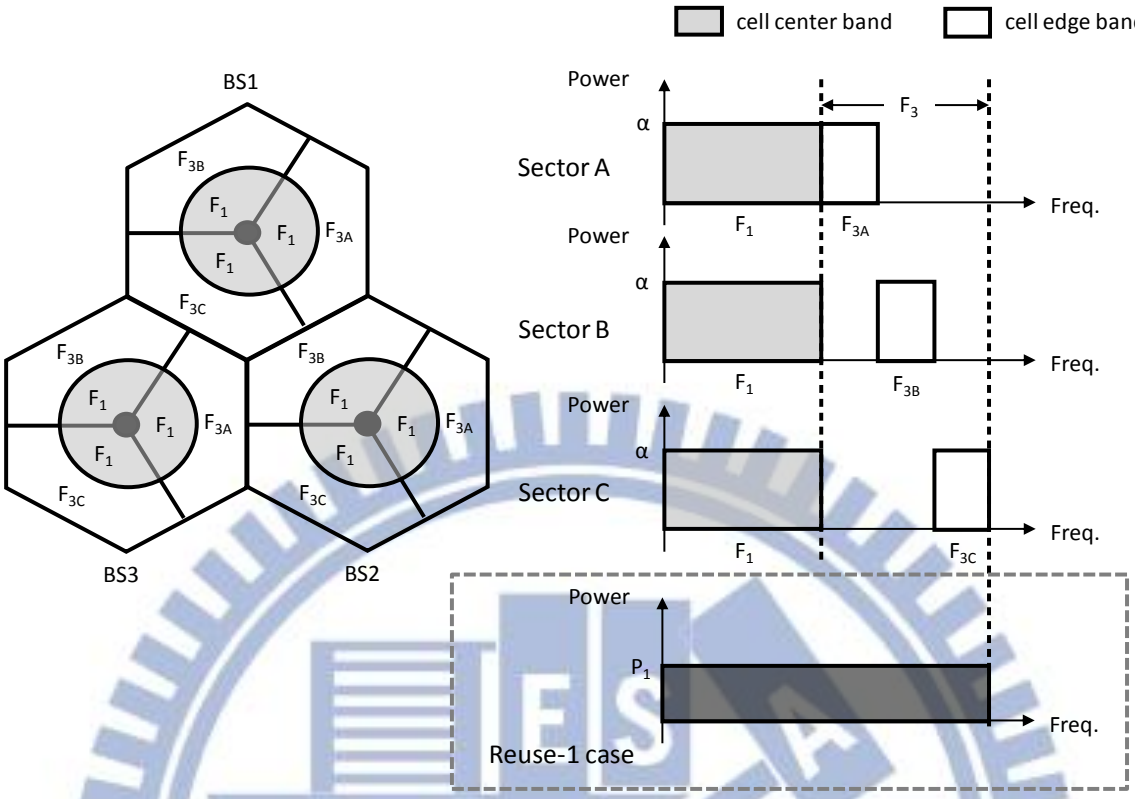

Fig. 2-1 Spectrum setting for PFR in a tri-sector cellular layout

2.2.2 Soft Frequency Reuse

Soft frequency reuse (SFR) is an ICIC that works in a power coordination manner. Since all frequency resources are reused in every cell (see Fig. 2-2), the effective frequency reuse factor is still one. In soft frequency reuse, for a tri-sector cellular layout, the whole frequency band is divided into three subbands in every cell, one subband (e.g. $F_{A,E}$ in Fig. 2-2) is called cell edge band, on which the transmission power is amplified, and the other two subbands (e.g. $F_{A,C1}$ and $F_{A,C2}$ in Fig. 2-2) are termed as cell center band. Note that each cell edge band occupies one third of the whole frequency resource and is orthogonal to the cell edge bands of the neighboring cells. The cell edge users are better served in the high power band, since they could have better signal power and reduced inter-cell

interference. Therefore, when applying the SFR scheme, the cell edge users are primarily scheduled on the cell edge band (i.e. high power band), while users closer to their serving cell site have exclusive access to the cell center band (i.e. low power band) and could also use the cell edge band if it is not taken by the cell edge users.

Figure 2-2 illustrates a standard power mask setting for SFR in a tri-sector cellular layout, in which three power masks, namely power mask *type-A*, *type-B*, and *type-C*, are applied to three cells of the same site (i.e. base station). We assume that the transmit power is equally spread over the cell edge/center bands individually in each cell. By denoting the power level (or power spectrum density) on cell edge and cell center bands as P_{edge} and P_{center}, respectively, a power amplification factor (PAF) β is given to represent the power ratio of cell edge band to cell center band and it can be defined as

$$\beta = \frac{P_{edge}}{P_{center}} \quad (>1 \text{ in SFR}). \tag{2-4}$$

Moreover, by assuming constant total power, if we denote the power level in a reuse-1 system as P_1 (see Fig. 2-1), then the power level P_{edge} and P_{center} can be obtained by (2-5) and (2-6), respectively.

$$P_{edge} = \frac{3 \cdot \beta}{\beta + 2} P_1 \tag{2-5}$$

$$P_{center} = \frac{3}{\beta + 2} P_1 \tag{2-6}$$

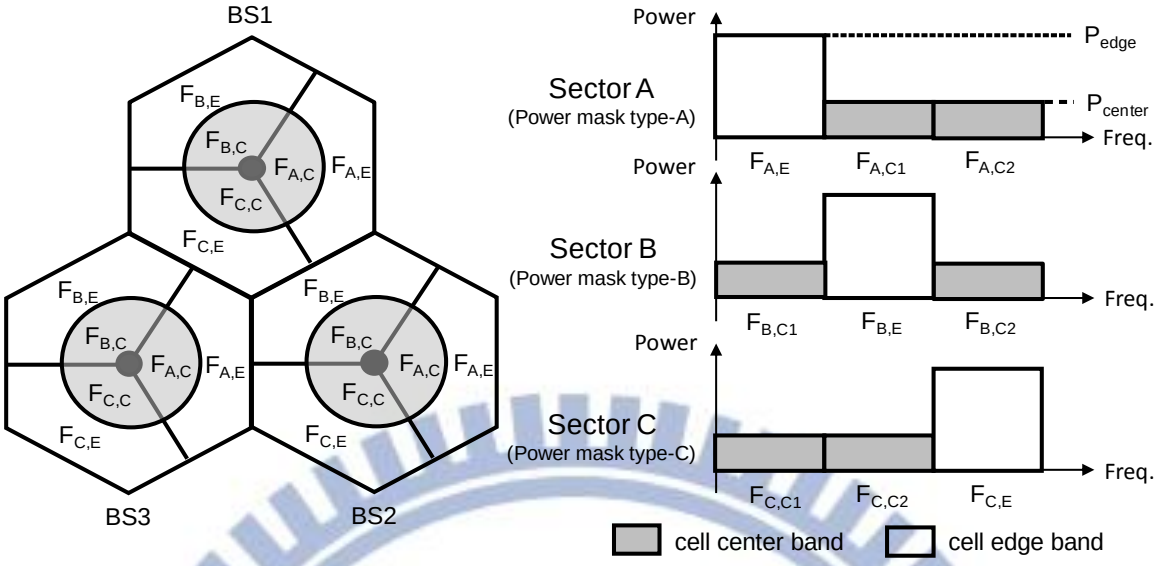

Fig. 2-2 Power mask for SFR in a tri-sector cellular layout

2.3 SSD-Based User Grouping Method

In order to perform PFR and SFR schemes, it is essential to distinguish between cell interior users (CIUs), which have a low probability to interfere with neighbor cells, and cell edge users (CEUs), which have a high probability to interfere with neighbor cells. Recently, the signal strength difference based (SSD-based) user grouping method is considered as a feasible and suitable solution in OFDMA downlink systems for ICIC applications. This is because the method is based on the existing handover measurements available in UMTS (Universal Mobile Telecommunication System), and it does not require additional signaling. Accordingly, SSD-based method has been recommended by 3GPP for ICIC operations in LTE system, in which the average received signal strength (RSS) or path gain measurement used in handover is used for the identification of interior users/edge users. For handover purpose with the SSD-based method, each UE needs to do downlink average RSS measurements from the serving cell as well as the neighboring cells. In the

SSD-based user grouping method, an UE is identified as a cell edge user when at least one of its surrounding cells provides average RSS which is within a threshold (difference) value (δ_{SSD}, in dB) from the highest average RSS, i.e. the average RSS of the serving cell. When an UE "sees" more than one cell, it usually faces a coverage problem and it is very reasonable for the system to classify it as a CEU.

For ease of understanding, we give the following example. Suppose the average RSS (in dB scale) measurements for an UE are ranked in descending order as $\overline{RSS}_s \geq \overline{RSS}_1 \geq \overline{RSS}_2 \geq \cdots$, in which $\overline{RSS}_i$ (i=1,2,…) denotes the i-th largest *average RSS* among the neighboring (or interfering) cells measured by the UE and $\overline{RSS}_s$ is the average RSS of the serving cell. Then, this UE will be treated as a cell edge user if $\overline{RSS}_s - \overline{RSS}_1 \leq \delta_{SSD}$ (in dB); otherwise, it will be treated as a cell interior user. Note that average RSS is a long-term measurement taking into account of transmit power, distance-dependent path loss, shadowing and antenna gain; and further, it can be acquired by observing received reference signal or pilot signal power of the serving cell and each surrounding cell.

2.4 Analysis of Cell Capacity

Generally, ICIC schemes may be static or semi-static with respect to the time scale of reconfiguration [38]. In this work, we consider the static coordination scheme for which the coordination is performed during the network planning stage. Although a static coordination would be a sub-optimal solution, it is highly recommended due to its simplicity [39, 40]. Furthermore, we assume all frequency resources designated for each cell are fully utilized (i.e. a fully loaded system).

2.4.1 Average SINR Modeling for Partial Frequency Reuse

Here, we do not consider fast fading and assume radio link is subject to propagation loss and log-normally distributed shadowing. As we have equal power allocation assumption for PFR scheme, the transmission power spectrum density P_t (or transmit power level α, see Fig. 2-1) is given by

$$P_t = (P_T / BW_{all}) \cdot r_{eff} \; (= P_T / BW_{cell}), \tag{2-7}$$

where P_T denotes total transmission power. Thus, the average SINR for an UE can be written as

$$\gamma^{(x)} = \frac{P_t \cdot L_s \cdot S_s \cdot A_s}{\sum_{i \in \Phi_x} P_t \cdot L_i \cdot S_i \cdot A_i + P_N}, \; (x = 1, 3) \tag{2-8}$$

where L_j, S_j, and A_j are the pathloss, shadow fading and antenna gain from the cell j to the UE, respectively; the subscripts s and i stand for the serving cell and the interfering cells, respectively; Φ_1 and Φ_3 are the sets of interfering cells with a reuse factor of 1 and a reuse factor of 3, respectively; P_N denotes the received noise power spectrum density. Recall that the serving cell is the one from which the *average received signal strength* ($\overline{RSS}$) is the strongest. Let γ_I and γ_E be the average received SINR of the CIU and CEU, respectively, obviously we have $\gamma_I = \gamma^{(1)}$ and $\gamma_E = \gamma^{(3)}$.

2.4.2 Average SINR Modeling for Soft Frequency Reuse

Without loss of generality in the average SINR calculations of SFR scheme, we

consider the case in which an UE is served by a cell with power mask *type-A*. In this case, when the UE is a cell edge user, its average SINR is given by

$$\gamma_E = \frac{P_{edge} \cdot L_s \cdot S_s \cdot A_s}{\sum_{i \in \Phi_A} P_{edge} \cdot L_i \cdot S_i \cdot A_i + \sum_{i \in \Phi_B} P_{center} \cdot L_i \cdot S_i \cdot A_i + \sum_{i \in \Phi_C} P_{center} \cdot L_i \cdot S_i \cdot A_i + P_N}, \tag{2-9}$$

where subscripts *s* and *i* again stand for the serving cell and the interfering cells, respectively; Φ_A, Φ_B and Φ_C are the sets of interfering cells with power mask *type-A*, *type-B* and *type-C*, respectively.

On the other hand, when the UE is a cell interior user, there are two possible subbands for the UE to operate on, one is $F_{A,C1}$ and the other one is $F_{A,C2}$. Let γ_I^{C1} and γ_I^{C2} denote the corresponding average SINRs on subband $F_{A,C1}$ and subband $F_{A,C2}$, respectively. Referring to Fig. 2-2, they can be expressed as

$$\gamma_I^{C1} = \frac{P_{center} \cdot L_s \cdot S_s \cdot A_s}{\sum_{i \in \Phi_A} P_{center} \cdot L_i \cdot S_i \cdot A_i + \sum_{i \in \Phi_B} P_{edge} \cdot L_i \cdot S_i \cdot A_i + \sum_{i \in \Phi_C} P_{center} \cdot L_i \cdot S_i \cdot A_i + P_N}, \tag{2-10}$$

$$\gamma_I^{C2} = \frac{P_{center} \cdot L_s \cdot S_s \cdot A_s}{\sum_{i \in \Phi_A} P_{center} \cdot L_i \cdot S_i \cdot A_i + \sum_{i \in \Phi_B} P_{center} \cdot L_i \cdot S_i \cdot A_i + \sum_{i \in \Phi_C} P_{edge} \cdot L_i \cdot S_i \cdot A_i + P_N}. \tag{2-11}$$

Assuming that each cell interior UE can choose the subband on which the average SINR is maximum, we can further obtain the average SINR of a cell interior UE as in (2-12).

$$\gamma_I = \max\left(\gamma_I^{C1}, \gamma_I^{C2}\right) \tag{2-12}$$

2.4.3 Modified Shannon Formula

According to Shannon's capacity formula [41], the achievable link spectral efficiency *C* (bps/Hz) from a BS to a particular user is a function of the average received SNR (signal to noise ratio) and can be written as

$$C(SNR) = \log_2(1 + SNR). \tag{2-13}$$

In general, Shannon's formula gives the capacity of an additive white Gaussian noise (AWGN) channel and it is not applicable to a multipath channel. Assume that other-cell interference can be modeled as AWGN and we do not consider other-cell interference cancellation techniques in the receiver, a modified Shannon formula has been introduced in [42] to calculate link capacity in a cellular mobile radio communication system. This formula is given as

$$\tilde{C}(\gamma) = \xi \cdot \log_2(1 + \gamma / \varsigma),\ (bps/Hz) \tag{2-14}$$

where ξ and ς are constants that account for the system bandwidth efficiency and the SINR implementation efficiency, respectively, and γ denotes the long-term average received SINR, i.e. *G-factor*. For Typical Urban (TU) channel model and Single-Input Single-Output (SISO) antenna scheme, it has been shown in [42] that Equation (2-14) with $\xi = 0.56$ and $\varsigma = 2$ achieves a good match to the link capacity performance of 3GPP LTE from simulation. Therefore, we adopt this modified Shannon capacity equation with parameters $\xi = 0.56$ and $\varsigma = 2$ to evaluate the link spectral efficiency.

2.4.4 Throughput Calculation

We assume that the users are uniformly distributed within cell coverage, and each user has unlimited traffic to transmit on the downlink. Moreover, it is assumed that a *Round Robin* (RR) scheduler is applied to cell center/edge bands. Under the RR scheduling policy, the system capacity *T* can be calculated as [42, 43]

$$T = BW \cdot \nu \cdot \int \tilde{C}(\gamma) f_{\gamma}(\gamma) d\gamma \,, \tag{2-15}$$

where ν is a loss factor that accounts for the system overhead, $f_{\gamma}(\gamma)$ is the probability density function of SINR γ, and *BW* denotes the allocated bandwidth. In this work, the loss factor ν is set to 1; this yields optimistic results, but is deemed acceptable for relative comparison purposes.

In a fully loaded system, it becomes unlikely that CIUs would be able to access the cell edge band, and they would thus be confined to the cell center band. This causes a separation of user groups for which the CIUs occupy the cell center band only while the CEUs use the cell edge band only. From (2-15), the average cell interior throughput and cell edge throughput for the PFR can be calculated by (2-16) and (2-17), respectively,

$$T_{Interior} = BW_{F_1} \cdot \int \tilde{C}(\gamma_I) f_{\gamma_I}(\gamma_I) d\gamma_I \,, \tag{2-16}$$

$$T_{Edge} = \frac{1}{3} BW_{F_3} \cdot \int \tilde{C}(\gamma_E) f_{\gamma_E}(\gamma_E) d\gamma_E \,, \tag{2-17}$$

in which the subscripts *I* and *E* stand for the CIUs and CEUs, respectively.

And, for the SFR scheme, the corresponding throughput metrics can be calculated by (2-18) and (2-19), respectively. We recall that BW_{all} denotes the whole system bandwidth

since SFR enables frequency reuse one.

$$T_{Interior} = \frac{2}{3} BW_{all} \cdot \int \tilde{C}(\gamma_I) f_{\gamma_I}(\gamma_I) d\gamma_I \tag{2-18}$$

$$T_{Edge} = \frac{1}{3} BW_{all} \cdot \int \tilde{C}(\gamma_E) f_{\gamma_E}(\gamma_E) d\gamma_E \tag{2-19}$$

After obtaining the average throughput of the cell interior users and cell edge users, the average cell throughput (T_{Cell}) thus becomes

$$T_{Cell} = T_{Interior} + T_{Edge}. \tag{2-20}$$

2.5 Numerical Results and Discussions

2.5.1 Simulation Setup, Assumptions and Calibration

Two types of macro-cell scenarios for inter-site distances (ISDs) of 500m and 1732m defined by 3GPP are considered in this work. Following the terminology used in 3GPP [44], we refer to the scenarios as *Case 1* and *Case 3* for ISD=500 m and ISD=1732m, respectively. Static snapshot simulations have been used. The average SINR distribution is obtained through Monte Carlo simulations involving 2000 random placement of users geographically. The available downlink bandwidth is fixed at 10 MHz. We consider a multi-cell (hexagonal cellular) system consisting of 19 base stations (BSs), and each BS controls three sectors (cells), i.e., 57 sectors (cells) in total are simulated. Simulation assumptions and parameters basically follow the 3GPP evaluation criteria [44]. The radio links are subject to distance-dependent propagation loss and lognormal shadow fading. A distance-dependent path loss with a propagation loss exponent of 3.76 and a lognormal

shadowing with a standard deviation of 8 dB are assumed. The sector antenna pattern used in our simulation is adopted from [44]. All the simulation results are collected from the three sectors of the central BS and the remaining 54 sectors act as inter-cell interference sources. The simulation parameters and assumptions are summarized in Table 2-1.

Herein, we show wideband (long-term) average SINR (i.e. *G-factor*) distribution that obtained from our simulation results and that published by 3GPP [45] in Fig. 2-3 and Fig. 2-4, respectively. From the figures, we can observe that our simulated average SINR distribution fit very well with the 3GPP's results, and this implies that our simulation platform is a trustworthy one.

Table 2-1 Simulation parameters and assumptions

Parameters	Assumptions
Cellular layout	Hexagonal grid, 19 BSs, 3 cells per BS
Carrier Frequency	2 GHz
System bandwidth	10 MHz
Antenna pattern	As described in [44]
BS total Tx power	46 dBm
Inter -site distance (ISD)	500 m, 1732 m
Distance dependent path loss	$128.1+37.6\log_{10}(R)$, R in km
Minimum distance between UE and cell site	35 m
Penetration loss	20 dB
Shadowing standard deviation	8 dB
Correlation distance of shadowing	50 m
Shadowing correlation between BSs / sectors	0.5 / 1
BS antenna gain	14 dBi
UE antenna gain	0 dBi
UE noise figure	9 dB
Antenna configuration	1 x 1

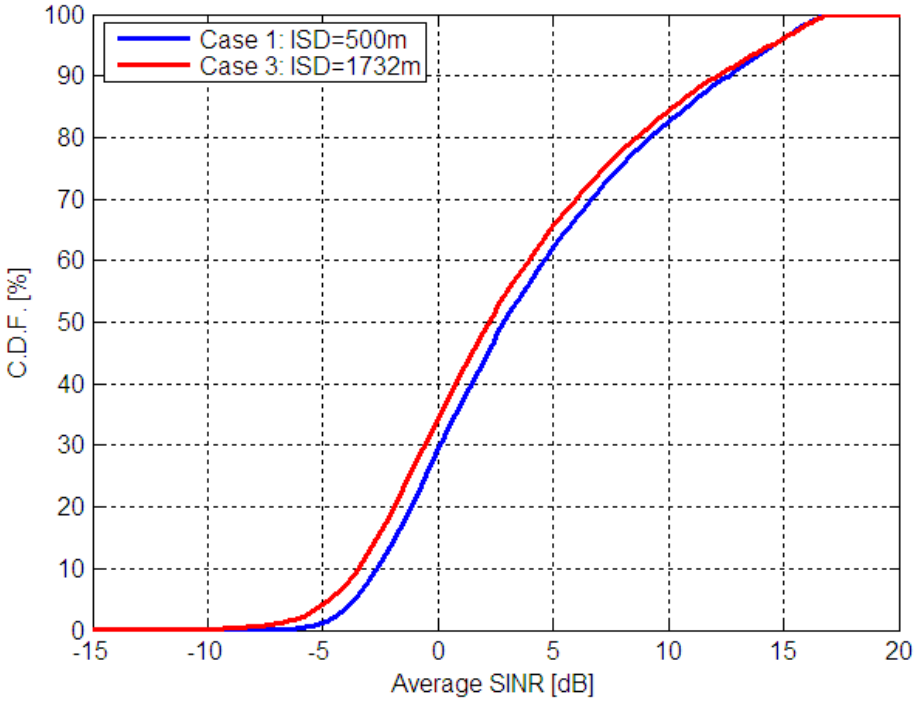

Fig. 2-3 Average SINR (*G-factor*) distribution for 3GPP *Case 1* and *Case 3* (our results)

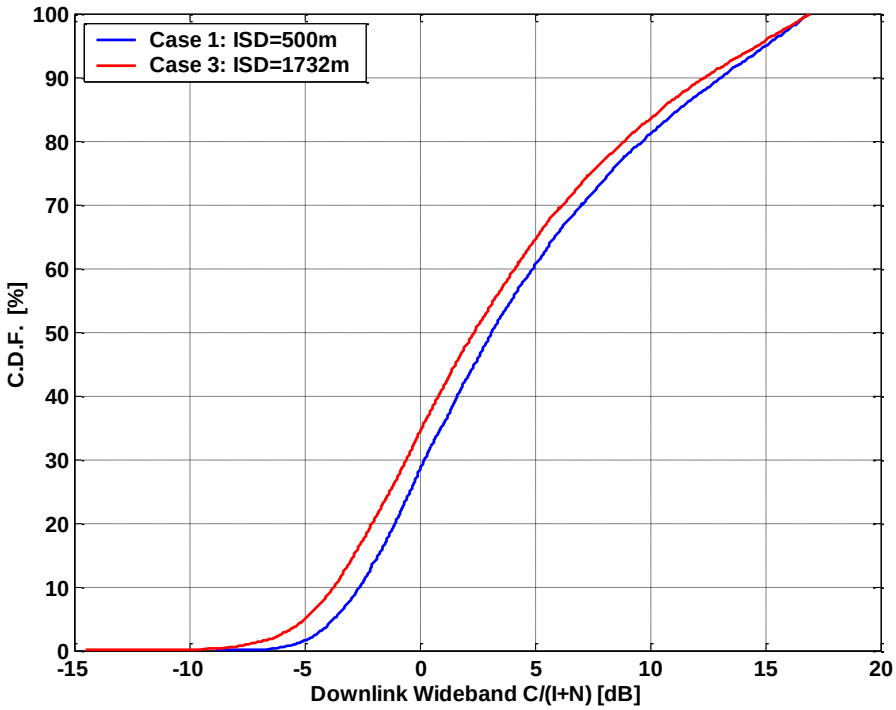

Fig. 2-4 Average SINR (*G-factor*) distribution for 3GPP *Case 1* and *Case 3* (3GPP's results)

2.5.2 Percentage of Cell Edge Users

For ICIC operation, the user types classification threshold δ_{SSD} should be large enough to include a sufficient number of users with low SINR; however, in order to avoid an excess of uplink signaling overhead (caused by UE measurement reports), this value should not be too large. In this paper, a classification threshold (δ_{SSD}) of 3dB is adopted [46, 47]. Note that coordinated multi-point (CoMP) technique [15], which is proposed for 3GPP LTE-Advanced to mitigate inter-cell interference and to increase cell edge throughput, also employs the SSD-based method for the decision on CEUs; and further, since $\delta_{SSD} = 3\text{dB}$ is commonly used for CoMP evaluations, hence it should be a good working assumption in this work. Figure 2-5 plots the percentage of CEUs within a cell as a function of the threshold δ_{SSD}. It is observed that as δ_{SSD} increases, there are more UEs being marked as CEUs. Also as shown in Fig. 2-5, assuming $\delta_{SSD} = 3\,\text{dB}$, the percentage of edge users within a cell is about 25%, and thus the corresponding percentage value for CIUs is about 75%. Since relative signal strength remains unchanged even if inter-site distance is changed, the percentages of CEUs and CIUs within a cell for the two interested deployment scenarios (i.e., ISD=500m and ISD=1732m) are the same.

2.5.3 Results of Capacity Estimation

To begin with, we illustrate the performance of reuse-1 scheme as a reference since universal frequency reuse (i.e. reuse-1) is being targeted for next generation OFDMA systems. Figure 2-6 shows the average throughput performance for reuse-1 deployment. Here we can see that due to smaller cell size, *Case 1* scenario achieves higher system capacity as compared with *Case 3*.

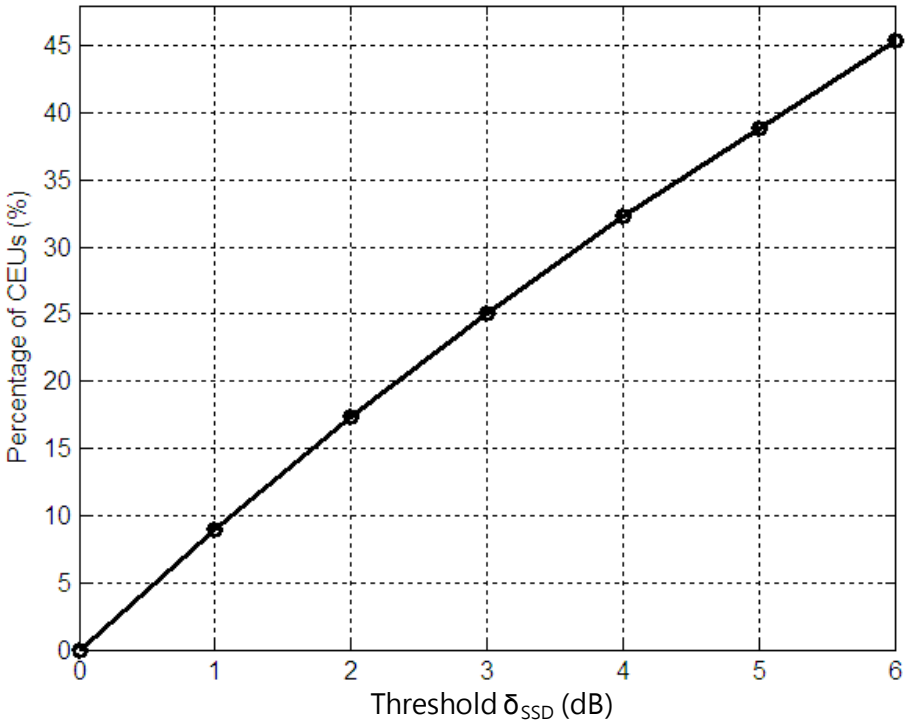

Fig. 2-5 Percentage of cell edge users under SSD-based user grouping method

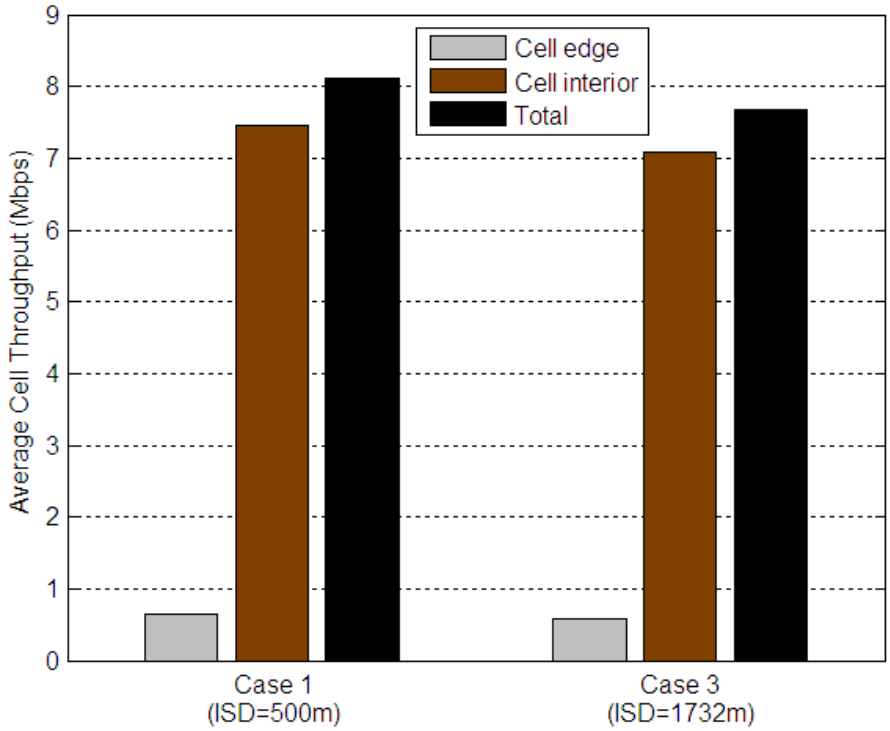

Fig. 2-6 Average throughput performance of the reuse-1 scheme in 3GPP *Case 1* and *Case 3* Scenarios

We plot in Fig. 2-7 the average cell throughput (T_{Cell}), cell interior throughput ($T_{Interior}$) and cell edge throughput (T_{Edge}) for the PFR scheme as a function of the effective reuse factor (ERF) and we also plot the performance of reuse-1 as a reference. It can be seen that as the ERF increases, there is a significant increasing trend for cell edge throughput. However, this improvement is at the cost of throughput degradation in the central area, and this further leads to a reduction of total cell throughput. This is because as the ERF increases, the amount of frequency resources available on cell edge band is increased, which leaves more system bandwidth unused. Furthermore, we find that the PFR scheme can improve the cell edge throughput remarkably as compared with the reuse-1 scheme, but a loss of total cell throughput occurs when the ERF is larger than 1.28 and 1.25, respectively, for *Case 1* and *Case 3* scenarios. In addition, it is worthy of note that the cell edge throughput gain is more pronounced for *Case 1* scenario (i.e. small cell size scenario). For example, considering the case that the ERF is equal to 1.3, the PFR scheme improves the reuse-1 scheme by approximately 120% and 80% in edge throughput for *Case 1* and *Case 3* scenarios, respectively; however, the corresponding total cell throughput losses are about 2.5% and 4.5%.

Figure 2-8 shows the cell throughput performance for the SFR scheme as a function of the power amplification factor (PAF) and the results of reuse-1 are also plotted. Again, similar performance trends can be drawn from the results. It can be seen that the larger PAF we employ, the more cell edge throughput gain can be obtained; nevertheless, the total cell throughput is decreased as the PAF increases. This is due to the fact that boosting the power on the cell edge band not only lowers the transmitted power level on the remaining two-thirds of the bandwidth (i.e., cell center band), but it also causes strong interference to neighboring cells, and as a result, introduces overall throughput degradation. Furthermore, comparing with the reuse-1 scheme, we see that the SFR scheme can enhance cell edge

performance at the cost of overall capacity degradation. For example, when the PAF is equal to 2, it is observed that while the SFR scheme achieves about 110% improvement in cell edge throughput with respect to the reuse-1 scheme, it suffers from total cell throughput degradation by approximately 12%. It is worthy to note that these values are about the same for both *Case 1* and *Case 3* scenarios. In summary, we conclude that both PFR and SFR schemes are very effective ways to ameliorate cell edge performance; however, it is very important to choose a proper ERF and PAF, respectively, for PFR and SFR schemes with which the performance of cell boundary users will be improved as much as possible while that of the inner region of cell will not be degraded too much.

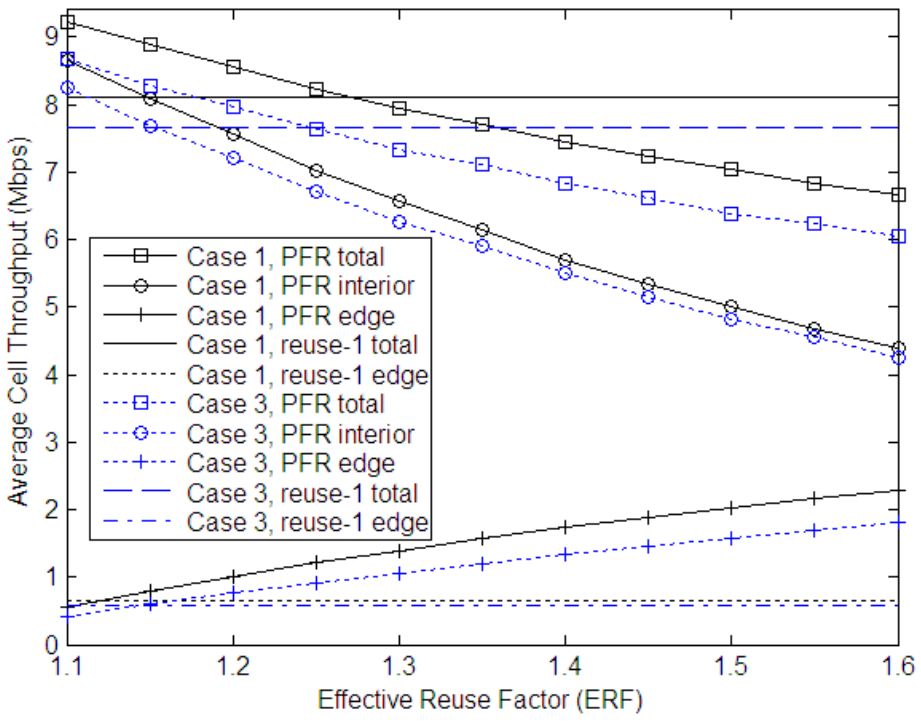

Fig. 2-7 Average throughput performance of the partial frequency reuse scheme in 3GPP *Case 1* and *Case 3* Scenarios

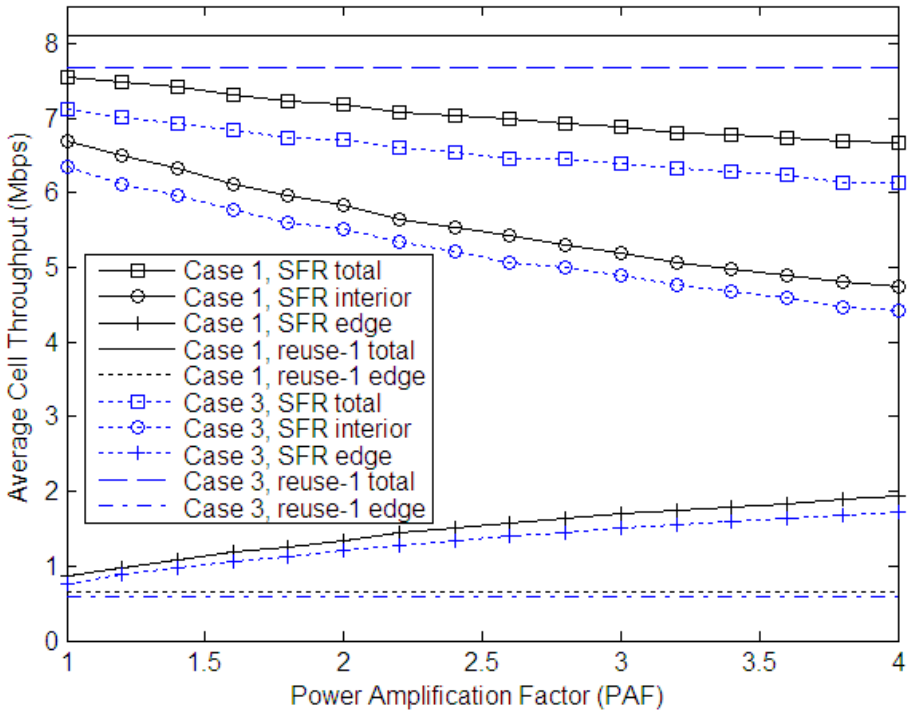

Fig. 2-8 Average throughput performance of the soft frequency reuse scheme in 3GPP *Case 1* and *Case 3* Scenarios

2.5.4 System Capacity Comparison between PFR and SFR

In a mobile communication system, data-rate fairness among users is an important requirement to take into account. Herein, we introduce a parameter *f*, called *data-rate fairness index*, as the ratio of the average CIU throughput to the average CEU throughput, and it can be written as

$$f = \frac{T_{Interior}/(N_u \cdot Pb_I)}{T_{Edge}/(N_u \cdot Pb_E)}, \tag{2-21}$$

where N_u denotes the number of active users in one cell; Pb_I and Pb_E are the (statistical) probability of CIUs and CEUs, respectively. Note that by assuming $\delta_{SSD} = 3\,\text{dB}$, we have

shown that Pb_I=0.75 and Pb_E=0.25. In this work, two data-rate fairness cases are studied [37]: the first one is f=1, which is called *fair*; the other one is f=2, which is called *less fair*. To start with, we choose the ERFs and PAFs, which can fulfill the predefined fairness criteria, for PFR and SFR schemes, respectively. According to our simulation results, the selected ERFs (PAFs) that can closely achieve *fair* and *less fair* for *Case 1* scenario are 1.43 (3.1) and 1.24 (1.4), respectively, and the corresponding factors for *Case 3* scenario are 1.50 (3.5) and 1.29 (1.5), respectively.

Figure 2-9 and Fig. 2-10 demonstrate the average cell throughput vs. data-rate fairness performance for *Case 1* and *Case 3* scenarios, respectively. For comparison, the results of reuse-1 deployment are also shown in the figures. From the figures, we can have three observations. First, the better the data-rate fairness is, the lower the system throughput becomes, and this further demonstrates that there is a trade-off between system capacity and fairness. Second, the PFR scheme outperforms the SFR scheme in both *Case 1* and *Case 3* scenarios in spite of different fairness criterions being considered. In addition, we notice that the PFR scheme can provide more gains with the *less fair* case in the *Case 1* deployment scenario. This implies that the PFR scheme achieves fairer distribution of throughput at a lower cost as compared with the SFR scheme. For example, in *Case 1*, it is observed that the PFR scheme outperforms the SFR scheme by about 7% and 12% in cell throughput for *fair* and *less fair* cases, respectively. On the other hand, when we examine *Case 3*, these values are about 2% and 7% for *fair* and *less fair* cases, respectively. Finally, we find that in most cases, the reuse-1 scheme can yield superior system capacity, but suffers from fairness problems. However, as shown in Fig. 2-9, one can see that the PFR scheme achieves slightly better throughput than the reuse-1 scheme in the case of *less fair* under *Case 1* scenario. This shows that the throughput degradation due to accessible bandwidth loss caused by employing the PFR scheme can be regained, and it turns out to

be a small improvement in throughput. We notice that the value of the data-rate fairness index f is fixed with respect to reuse-1 scheme.

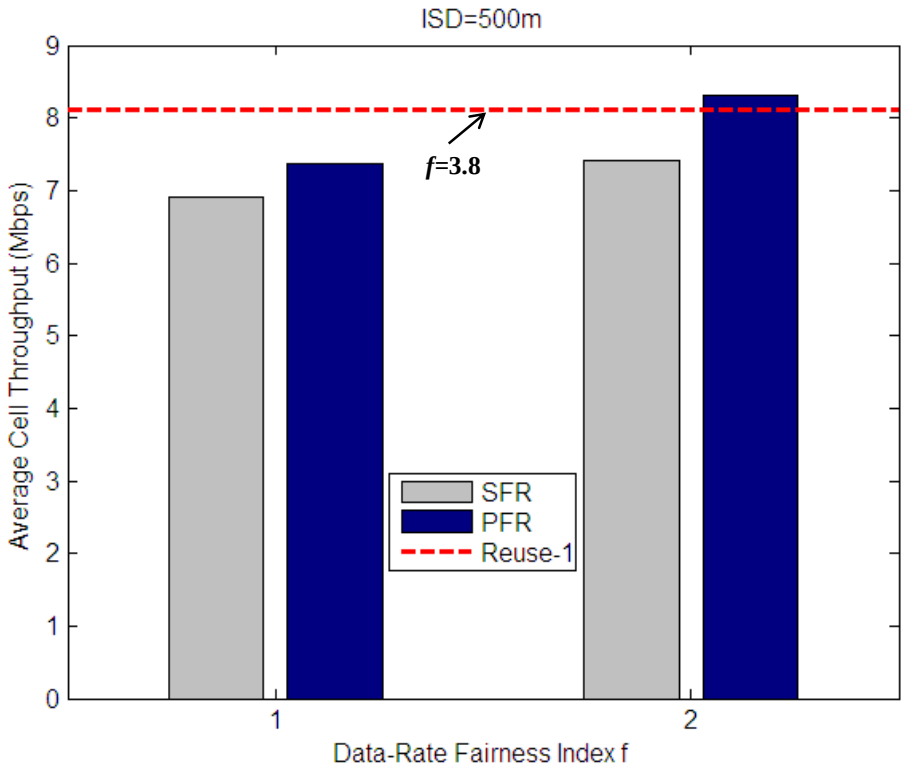

Fig. 2-9 System capacity vs. data-rate fairness under 3GPP *Case 1* scenario

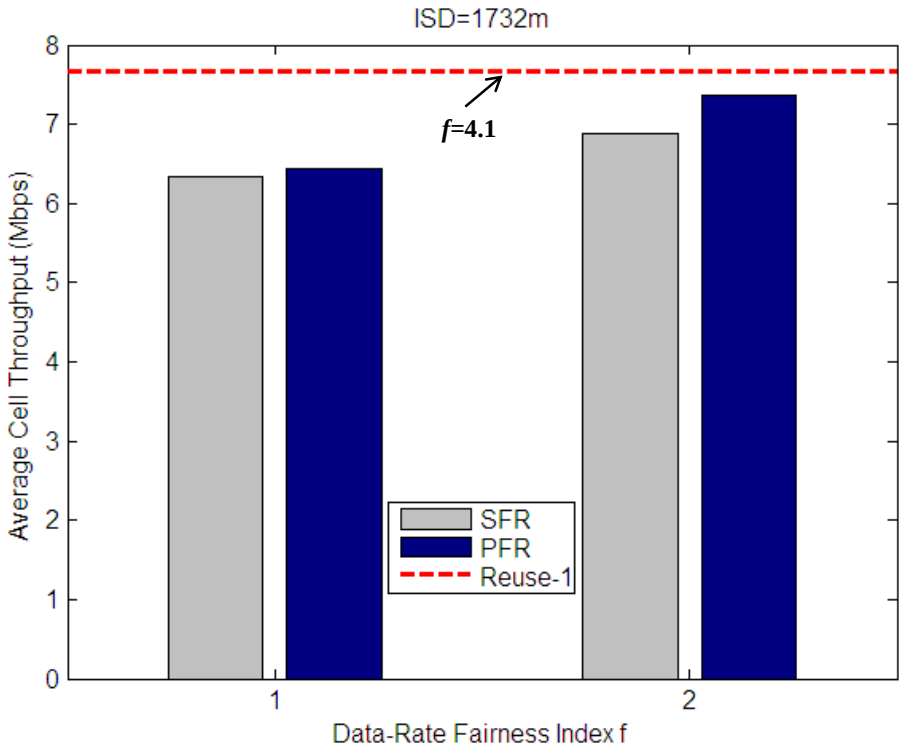

Fig. 2-10 System capacity vs. data-rate fairness under 3GPP *Case 3* scenario

2.6 Summary

To guarantee a quality of service for boundary users and more balanced data rate among users, PFR and SFR are widely used in next generation OFDMA systems for inter-cell interference mitigation. In this chapter, we investigate the throughput performance of PFR and SFR in a multi-cell OFDMA downlink system; and further, this work is specifically done by employing the SSD-based user grouping method, which is considered as a most promising approach and is currently adopted in 3GPP LTE system. Our simulation results show that both PFR and SFR can provide significant increases in throughput of cell edge users; however, this improvement is always at the cost of throughput of cell interior users, and as a result, total system capacity degradation occurred. Moreover, considering data-rate fairness among users, the results show that PFR

outperforms the SFR scheme in total cell throughput, and the gain is more pronounced with small cell size deployment scenario. In summary, we conclude that both PFR and SFR are very effective ways to cope with inter-cell interference in an OFDMA downlink system, but PFR is a more appropriate one to achieve data-rate fairness among users with having an acceptable system capacity.

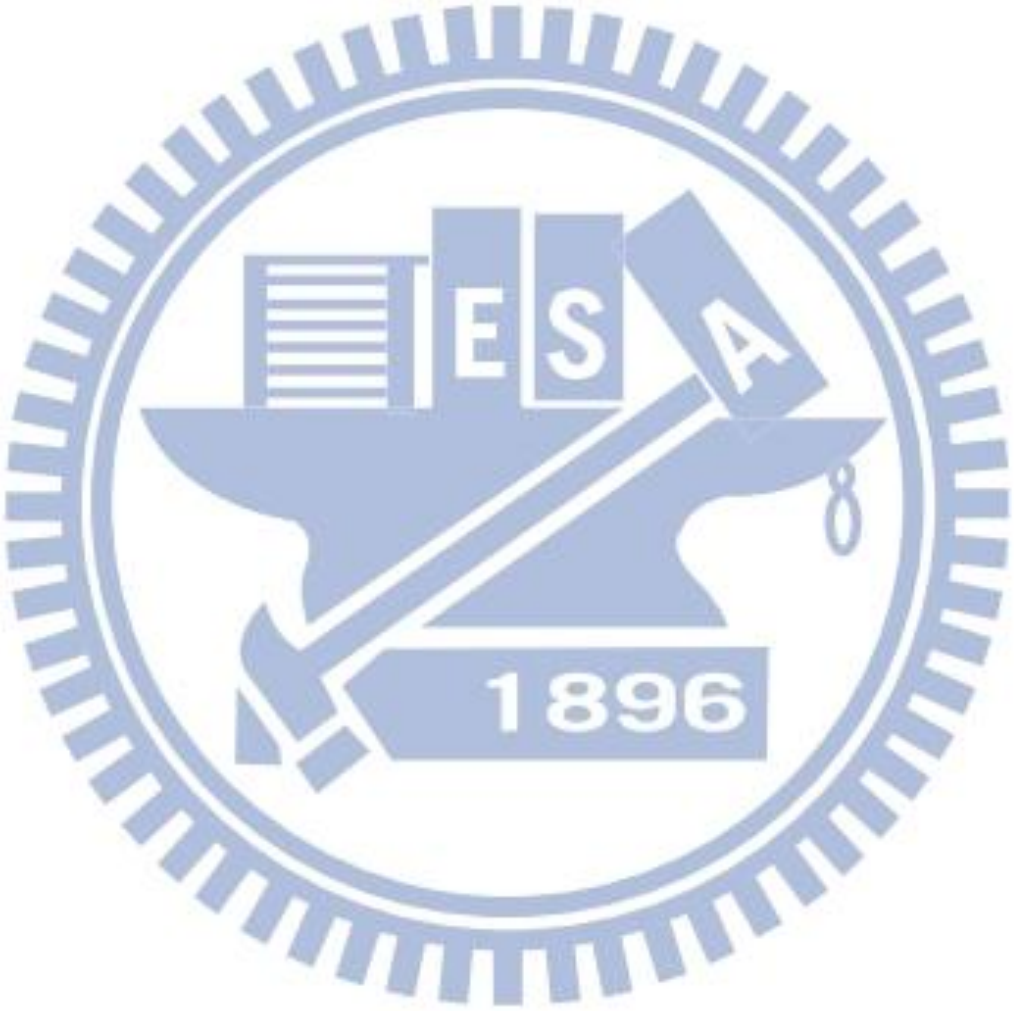

Chapter 3 A Hybrid Inter-cell Interference Mitigation Scheme for Cellular Homogeneous Networks

3.1 Introduction

Inter-cell interference coordination (ICIC) techniques which relies on resource management cooperation among cells, can effectively reduce inter-cell interference (ICI) effects especially in the cell-edge area. In the previous chapter, the performance of two widely used ICIC schemes, namely partial frequency reuse (PFR) and soft frequency reuse (SFR), were studied. And, according to the evaluation results, PFR scheme is seen as the most promising.

To improve radio coverage at cell borders in 3rd generation (3G) code division multiple access (CDMA) systems (e.g., WCDMA, cdma2000), soft handover which

exploits macro diversity has already been used to address the ICI problem. The signal transmission manner of soft handover in physical layer can be regarded as a kind of CoMP joint transmission (JT). Without considering higher layer (e.g. MAC, RLC) procedure for soft handover, soft handover scheme herein only spells the meaning of JT-like characteristics, i.e., the same data is conveyed from multiple cells/points. Besides soft handover, the processing gain in CDMA also helps to alleviate the cell edge interference problem. In order to maintain a simplified radio access network (RAN) architecture, it is agreed that soft handover will not be included in 3GPP LTE. Nevertheless, soft handover is supported in the Mobile WiMAX standard as an option (known as macro diversity handover in IEEE 802.16e-2005) [2]. Furthermore, it is worthy to note that CoMP JT will provide a natural framework for enabling soft handover in the LTE-Advanced system [18].

Conventionally, frequency reuse scheme is used in OFDMA, and soft handover scheme (exploiting macro diversity) in CDMA. In this chapter, we introduce a hybrid inter-cell interference mitigation scheme for an OFDMA downlink system. The proposed scheme makes use of both partial frequency reuse and soft handover. The motivation for developing this hybrid method is that, for a cell edge user, it is possible that a soft handover scheme may provide higher signal quality than a partial frequency reuse scheme and thus, it gives the possibility of improving cell edge bit rate. Simulation results show that this hybrid scheme can actually bring some capacity gains for the whole system as well as improve signal quality for cell edge users.

The rest of this chapter is organized as follows. In Section 3.2, we illustrate the soft handover scheme. In Section 3.3, we explain the proposed hybrid system concept. In Section 3.4, we present the system model, measures and assumptions for the performance evaluation. Our simulation results and discussions are given in Section 3.5. Finally, we give conclusions in Section 3.6.

3.2 Soft Handover Descriptions

One of the main macro diversity methods in 3G CDMA downlink is soft handover. It is well-known that exploiting macro diversity with a soft handover scheme is indeed a good method to reduce the influence of ICI and thus to increase the cell edge user data rate in cellular communication systems [48, 49]. When soft handover is in use, an UE is connected simultaneously to several cells (i.e. data information to the UE is simultaneously transmitted from *multiple* cells), which constitute its active set. An active set is the set of cells with which an UE is communicating at a given time. The active set includes the best cell (serving cell with highest path gain) and all the cells which satisfy the soft handover requirement, i.e., whose path gain are larger than the highest path gain minus the add threshold (Window_add [49]). Note that a soft handover scheme allows for more than one cell in the active set, while in a hard handover scheme, there is only one cell in the active set. In an OFDMA downlink system, with soft handover, the same signal is simultaneously transmitted to an UE from multiple cells through the same frequency subchannels (i.e. same time-frequency resources), as shown in Fig. 3-1. The benefit of soft handover comes from the fact that the dominant interferers become desired signals, and therefore, the cell edge transmission quality can be remarkably improved.

The soft handover overhead [49] is an important metric used to quantify the soft handover activity in a network, and it is regarded as a measure of additional transmission resources required. Note that a large soft handover overhead also implies a large number of control signaling and it decreases the system capacity. The soft handover overhead (ρ) is defined as

$$\rho = \sum_{n=1}^{N_{MAS}} n \cdot Pb_n - 1, \tag{3-1}$$

where N_{MAS} denotes the maximum active set size and Pb_n is the probability of an UE being in *n*-way soft handover. In this study, 1-way soft handover indicates the case that an UE is connected to only one cell, while 2-way soft handover indicates that the UE is connected to two cells, and so forth.

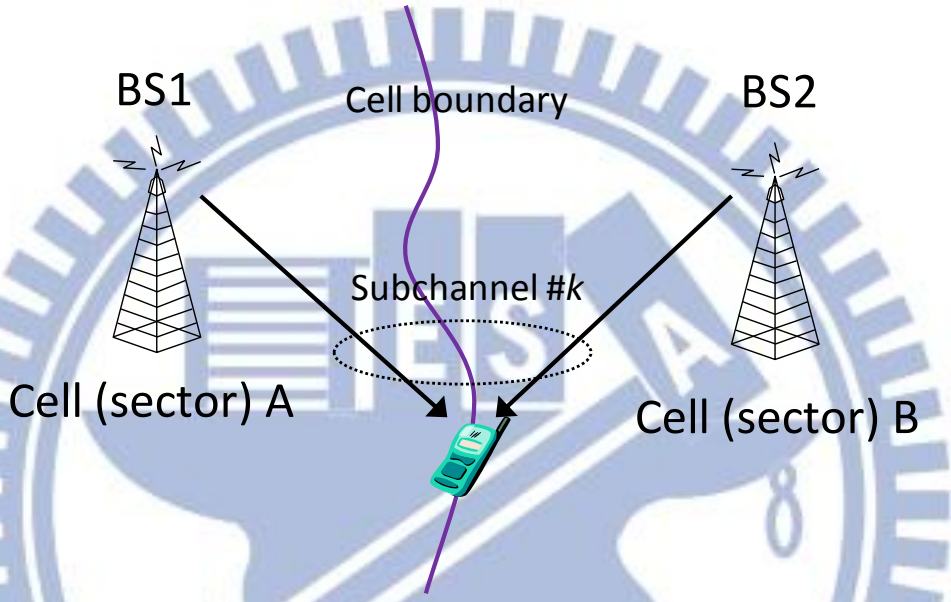

Fig. 3-1 The illustration of soft handover concept

3.3 A Hybrid System Concept

3.3.1 Cell Interior/Edge Users Partition

In the partial frequency reuse scheme, one part of the spectrum has a frequency reuse factor of 1 (reuse-1) and the other part has a frequency reuse factor of 3 (reuse-3). This spectrum partition works together with the split of users into cell interior users (CIUs) using the reuse-1 part of spectrum and cell edge users (CEUs) using the reuse-3 part of spectrum. Readers can refer to Section 2.2.1 for more details of partial frequency reuse

scheme.

For realizing the partial frequency reuse in an OFDMA system, we need to classify UEs into CIUs and CEUs. In this chapter, the widely accepted and used approach for research [26-30], which partitions UEs based on the geometry factor (*G-factor*), is adopted. Although SSD-based user grouping method is recommended by 3GPP LTE for ICIC operations, it would be rather a sub-optimal solution since some of the users with unfavorable signal quality would be left out. However, by adopting the G-factor based method, all the bad users (in terms of low SINR) can be selected from the system. And thus, it could indeed be a good method to use for relative comparison purposes. The G-factor is the wideband average SINR (signal to interference plus noise power ratio) measured by an UE from pilot subcarriers (or reference signals) over the reuse-1 part of the spectrum (F_1, see Fig. 2-1). The G-factor is then compared with a predefined threshold to determine whether the UE is a cell interior user or a cell edge user [12][26-30][50]. This is because a cell edge user always suffers from noticeable SINR degradation. The average SINR of an UE is defined as the ratio of totally received wideband own-cell power and other-cell interference plus noise power at the UE. It should be noted that the SINR is averaged over short-term fading, but not shadowing. In this paper, we consider an UE as a cell edge user which has to be protected by an inter-cell interference mitigation scheme, e.g., by a reuse-3 scheme or a soft handover scheme, if the G-factor measured at the UE is smaller than a threshold of 0 dB [26][30][50]; otherwise, the UE is regarded as a cell interior user.

3.3.2 Problem Formulation

We consider an OFDMA downlink system with partial frequency reuse; and further, we assume that soft handover (including softer handover) is supported. Assume that an UE is a cell edge user and there is more than one cell in the UE's handover list. The handover

list is the list of cells whose link quality satisfies the soft handover requirement, and thus every cell in the list can be added to active set. Note that the serving cell is certainly a member of the handover list, thus the size of handover list is always greater than or equal to one. In this situation, the OFDMA downlink system can use either of the following two methods to send the intended data to the UE. The first method is based on soft handover and the OFDMA downlink system sends data from all the cells that are in the UE's active set to the UE by using the frequency subchannels that belong to reuse-1 subband F_1 (see Fig. 2-1). We name this method *Scheme A*. The second method is based on partial frequency reuse (through a frequency reuse factor of 3) and the OFDMA downlink system sends data from the serving cell to the UE by using the frequency subchannels that belong to reuse-3 subband of the cell, i.e. F_{3A}, F_{3B}, or F_{3C} (see Fig. 2-1). We denote this method as *Scheme B*. Note that in *Scheme A*, the active set is exactly the set of cells in the handover list, and in *Scheme B*, the active set corresponds to only the serving cell.

In the above scenario, two remaining questions are: 1) Which scheme (*Scheme A* or *Scheme B*) could provide higher signal quality (SINR) for the UE? 2) As compared with the standard partial frequency reuse scheme (i.e. without soft handover option), can we generate some throughput gains by dynamically choosing between *Scheme A* and *Scheme B*? These two questions are addressed in the following sections.

3.3.3 A Hybrid System of Partial Frequency Reuse and Soft Handover

To enhance cell edge bit rate and overall system capacity, we develop an inter-cell interference mitigation scheme that dynamically chooses between *Scheme A* and *Scheme B* according to which scheme provides better signal quality (SINR). Figure 3-2 and Fig. 3-3 show the flow charts of the standard partial frequency reuse scheme and the proposed hybrid scheme, respectively. For the standard partial frequency reuse scheme (see Fig. 3-2),

a serving cell will first classify an UE as a CIU or a CEU according to the UE's G-factor. If the G-factor is greater than a predefined threshold (e.g., 0 dB in this paper), the UE is considered as a cell interior user and the serving cell will transmit the intended data to the UE through the frequency subchannels in the reuse-1 subband; otherwise, the UE is treated as a cell edge user and the serving cell will use the frequency subchannels with a reuse

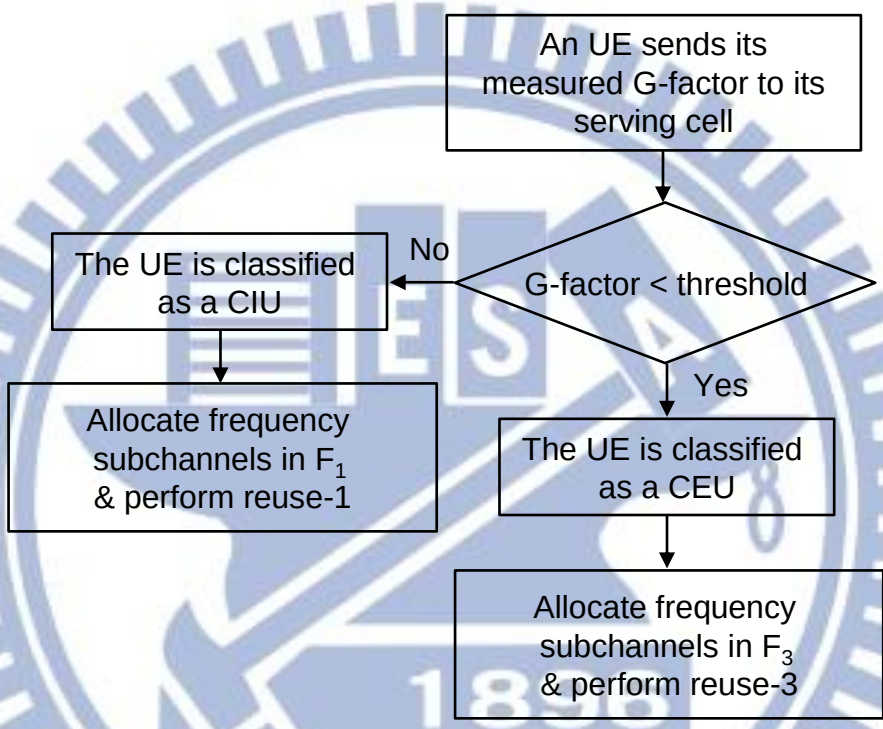

Fig. 3-2 Operational flow chat of partial frequency reuse scheme

factor of 3 (i.e. *Scheme B*) to send the intended data to the UE.

For the proposed scheme, a cell edge user may be allocated either frequency subchannels with a reuse factor of 3 or frequency subchannels with a reuse factor of 1 and use soft handover. Compare Fig. 3-2 with 3-3, we observe that the operations of CIUs are the same for both schemes. With Fig. 3-3, when an UE is classified as a cell edge user, the serving cell will use *Scheme B* to transmit the intended data to the UE if there is only one cell in the UE's handover list. On the other hand, if the UE's handover list size is larger

than one, then the serving cell will dynamically select either *Scheme A* or *Scheme B* to transmit the intended data to the UE and the selection criterion is based on signal quality comparison, which can be expressed as

$$\textit{If } \gamma_A^{(1)} > \gamma_B^{(3)}\textit{, choose Scheme A; otherwise, choose Scheme B.} \quad (3\text{-}2)$$

where $\gamma_A^{(1)}$ and $\gamma_B^{(3)}$ are the SINR measured by the UE with *Scheme A* (soft handover applied) and *Scheme B* (partial frequency reuse applied), respectively. Here, the superscript *x* (*x*=1 or 3) of $\gamma^{(x)}$ indicates that the SINR is measured on the reuse-*x* subband.

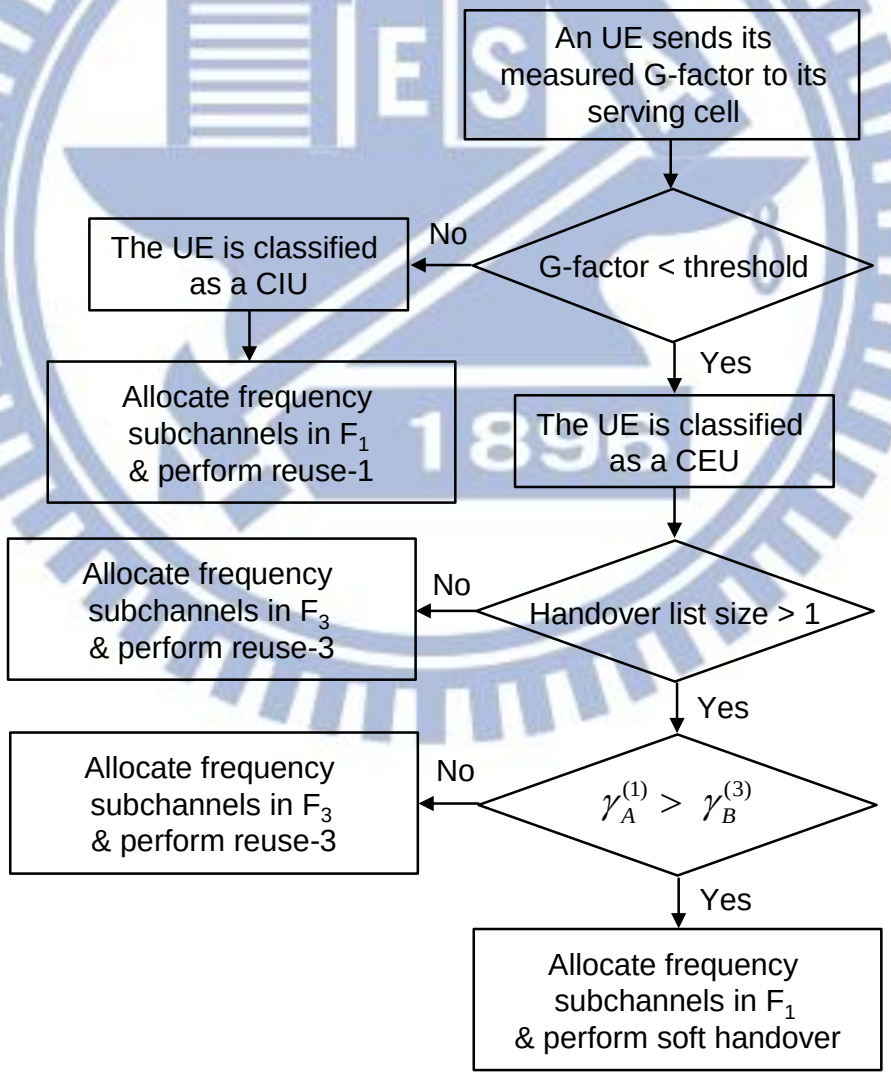

Fig. 3-3 Operational flow chat of the propose hybrid scheme

3.4 System Model, Measures and Assumptions

In this work, we operate PFR scheme in a static manner. Furthermore, we assume that the coordination message for soft handover (e.g. scheduling information, traffic data) can be exchanged between base stations without latency (or delay).

3.4.1 Modeling of downlink average SINR

In our SINR calculation, no fast fading modeling is considered and we suppose that each radio link is subject to propagation loss and log-normally distributed shadowing. We further assume that the serving cell is the one from which the received signal is the strongest after accounting for pathloss, shadow fading, and antenna gain patterns.

In each cell, we assume that all frequency subchannels are fully utilized (i.e. a fully loaded system) and transmit power is equally spread over the whole available bandwidth. Therefore, for a non-soft handover UE, its average SINR can be described as

$$\gamma^{(x)} = \frac{P_t \cdot L_s \cdot S_s \cdot A_s}{\sum_{i \in \Phi_x} P_t \cdot L_i \cdot S_i \cdot A_i + P_N}, \ (x = 1, 3) \qquad (3\text{-}3)$$

in which L_j, S_j, and A_j denote the pathloss, shadow fading and antenna gain from the cell j to the UE, respectively; the subscripts s and i stand for the serving cell and the interfering cells, respectively; Φ_1 and Φ_3 denote the sets of interfering cells with a reuse factor of 1 and a reuse factor of 3, respectively; P_N is the received noise power spectrum density. Note that in (3-3), P_t denotes the transmission power spectrum density and its expression can be found in (2-7).

Moreover, when the UE is in soft handover, its average SINR can be expressed by

$$\gamma_A^{(1)} = \frac{\sum_{s\in\Phi_{AS}} P_t \cdot L_s \cdot S_s \cdot A_s}{\sum_{i\in(\Phi_1-\Phi_{AS})} P_t \cdot L_i \cdot S_i \cdot A_i + P_N}, \tag{3-4}$$

where ϕ_{AS} denotes the active set of the UE and the subscript *s* here stands for the cells in the active set. In order to evaluate condition (3-2), we note that $\gamma_A^{(1)}$ can be calculated directly from (3-4) and $\gamma_B^{(3)}$ can be calculated by setting *x*=3 in (3-3).

3.4.2 System Capacity Estimation

The modified Shannon capacity formula has been illustrated in Section 2.4.3. In this chapter, once again, we adopt this modified Shannon capacity equation ($\tilde{C}(\gamma)$, see (2-14)), with parameters $\xi = 0.56$ and $\varsigma = 2$ to evaluate the link spectral efficiency.

Suppose the users are uniformly distributed within the cell's hexagonal area and a full queue traffic model is used for each user. Recall that a fully loaded network is assumed. By applying Round Robin (RR) scheduler to cell center/edge band, from (2-15) with $\nu = 1$, the average cell interior throughput ($T_{Interior}$) and cell edge throughput (T_{Edge}) for the partial frequency scheme can be written, respectively, as

$$T_{Interior} = BW_{F_1} \cdot \int \tilde{C}(\gamma_I) f_{\gamma_I}(\gamma_I) d\gamma_I, \tag{3-5}$$

$$T_{Edge} = \frac{1}{3} BW_{F_3} \cdot \int \tilde{C}(\gamma_E) f_{\gamma_E}(\gamma_E) d\gamma_E, \tag{3-6}$$

where the subscripts *I* and *E* stand for the CIUs and CEUs, respectively.

With the proposed hybrid scheme, as we have a RR scheduling policy on the cell center band, two user groups, the CIUs and the CEUs with *Scheme A*, will have equal chance of access to the frequency subchannels on the cell center band. Accordingly, the

average cell interior throughput and cell edge throughput can be obtained by (3-7) and (3-8), respectively,

$$T_{Interior} = BW_{F_1} \cdot \frac{Pb_I}{Pb_I + Pb_2 + Pb_3} \cdot \int \tilde{C}(\gamma_I) f_{\gamma_I}(\gamma_I) d\gamma_I \,, \tag{3-7}$$

$$T_{Edge} = \frac{1}{3} BW_{F_3} \cdot \int \tilde{C}(\gamma_{E,B}) f_{\gamma_{E,B}}(\gamma_{E,B}) d\gamma_{E,B} + \sum_{n=2}^{3} \left(\frac{1}{n} \cdot BW_{F_1} \cdot \frac{Pb_n}{Pb_I + Pb_2 + Pb_3} \cdot \int \tilde{C}(\gamma_{E,A,n}) f_{\gamma_{E,A,n}}(\gamma_{E,A,n}) d\gamma_{E,A,n} \right) , \tag{3-8}$$

in which Pb_I denotes the (statistically) probability of CIUs (ratio of CIUs to total users in number); Pb_n denotes the (statistically) probability of an UE being in n-way soft handover (that is the ratio of users with n-way soft handover to total users in number); and subscripts A and B represent *Scheme A* and *Scheme B* users, respectively. Note that in (3-8), $1/n$ that appears on the right hand side represents the capacity loss factor that is induced by performing a n-way soft handover. In this work, a maximum active set size of 3 cells ($N_{MAS} = 3$) [49] and an add threshold of 4 dB (Window_add = 4 dB) [51] are assumed.

Finally, the average (total) cell throughput (T_{Cell}) can be calculated as sum of the average throughput of the cell interior users and cell edge users, and it can be expressed by

$$T_{Cell} = T_{Interior} + T_{Edge} \,. \tag{3-9}$$

3.4.3 Simulation Method and Simulation Parameters

Table 3-1 lists the simulation parameters used in the evaluations, which basically follow the 3GPP evaluation criteria [44]. In the evaluation, we employ a three-sectored nineteen-hexagonal cell site layout model with the sector antenna beam pattern with a

70-degree beam width [44]. Static snapshot simulations have been adopted and the average SINR distribution (i.e. $f_\gamma(\gamma)$) is acquired through Monte Carlo simulations involving 2000 random placement of users geographically. We assume that the system bandwidth is fixed at 10 MHz and we set the inter-site distance to 1732 m. The locations of the UEs are randomly assigned with a uniform distribution within each cell. However, we set the minimum distance between a BS and a UE to 35 meters. The propagation model follows a distance-dependent path loss with the decay factor of 3.76 and lognormal shadowing with a standard deviation of 8 dB. The correlation values between the cell sites and that between sectors are 0.5 and 1.0, respectively. All the simulation results are collected from the three sectors of the central BS and the remaining 54 sectors act as a source of inter-cell interference.

Table 3-1 Simulation parameters and assumptions

Parameters	Assumptions
Cellular layout	Hexagonal grid, 19 BSs, 3 cells per BS
Carrier Frequency	2 GHz
System bandwidth	10 MHz
Antenna pattern	As described in [44]
BS total Tx power	46 dBm
Site to site distance	1732 m
Distance dependent path loss	$128.1+37.6\log_{10}(R)$ (R: in km)
Minimum distance between UE and cell site	35 m
Penetration loss	20 dB
Shadowing standard deviation	8 dB
Shadowing correlation between BSs / sectors	0.5 / 1
BS antenna gain	14 dBi
UE antenna gain	0 dBi
UE noise figure	9 dB
Antenna configuration	1 x 1

3.5 Numerical Results and Discussions

The simulation results are conducted for the standard partial frequency reuse (PFR) and the proposed hybrid scheme (PFR+SH). Furthermore, we consider the effective reuse factor (ERF) r_{eff} ranged between 1.1 and 2. For the definition of effective reuse factor, reader is referred to (2-1). Note that allocating a large number of frequency subchannels in the cell edge band will also cause a large loss in bandwidth utilization in each cell. Thus, we limit the effective reuse factor to 2, which in turn about 3/4 frequency resources are reserved for cell edge band F_3.

To begin with, it is beneficial to know the percentages of CIUs and CEUs in the simulation system. The cumulative distributed functions (CDFs) of downlink *G-factor* over the whole cell area are plotted in Fig. 3-4 for r_{eff} =1.2, 1.5, and 1.8. With a classification threshold of 0 dB, one can see that the percentage of CEUs within a cell is about 34% ($Pb_E \approx 0.34$) and that value for CIUs is about 66% ($Pb_I \approx 0.66$). Furthermore, since we assume that site-to-site distance is equal to 1732 m (see Table 3-1), the evaluation system will be interference limited, and thus one can find that the CDF is almost not changed with different effective reuse factors. Note that as compared with 3G mobile networks, the next generation mobile networks focus mainly on smaller cell size and ISD=1732m is the 3GPP working assumption for LTE evaluation.

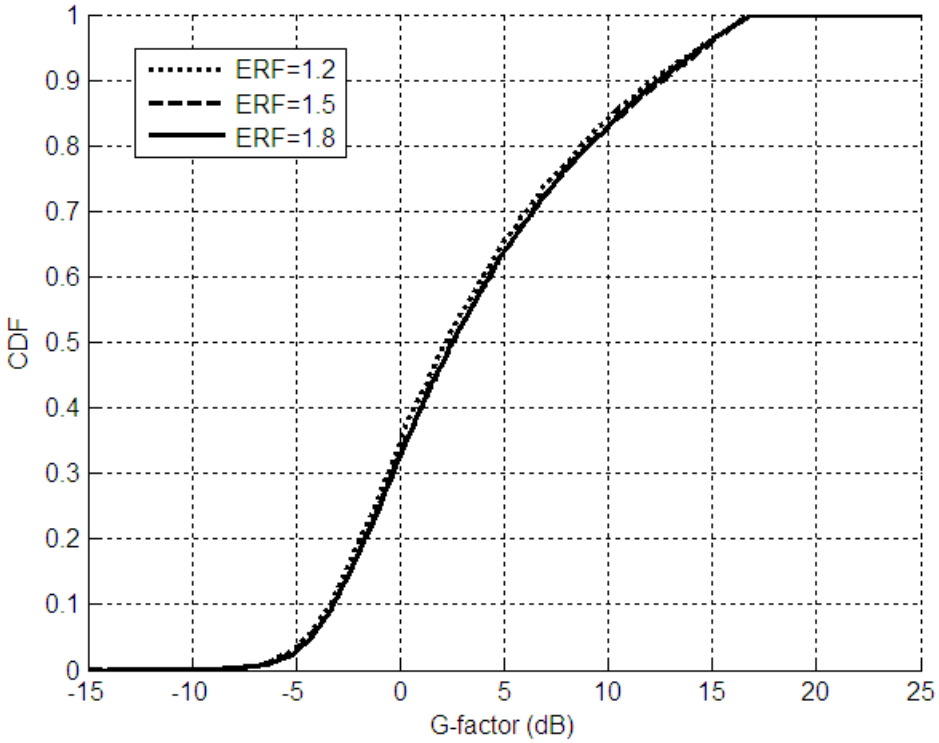

Fig. 3-4 G-factor distribution over cell area for different effective reuse factors

3.5.1 Soft Handover Overhead Estimation

Here, we study the soft handover overhead (ρ) of the proposed hybrid scheme. For feasibility reason, an important requirement of the PFR+SH scheme is to have a low soft handover overhead as compared with the current 3G CDMA systems. Table 3-2 shows the probability of an UE being in *n*-way soft handover (P_n) for the simulated system. Applying the simulation results to (3-1), we found that the induced soft handover overhead of the PFR+SH scheme is about 0.15. It is known that in a WCDMA network, the soft handover overhead is around 0.2-0.4 for a standard hexagonal cell grid with three sector sites [49]; and furthermore, in a live WCDMA network in a dense urban area, the typical value of the average overhead is about 0.38 [49]. Thus we conclude that the soft handover overhead of the simulated PFR+SH scheme is relatively small.

Table 3-2 Probability of an UE being in *n*-way soft handover (SH)

# of SH Branches	n =1	n=2	n=3
Pb_n	~0.91	~0.03	~0.06

3.5.2 Average SINR Comparison

Given a cell edge UE with $n \geq 2$ cells in its handover list, the probability that the received SINR of the UE with *n*-way (*n*=2, 3) soft handover (i.e. *Scheme A*) will be larger than that with a reuse-3 scheme (i.e. *Scheme B*) can be written as

$$Pb(n) = P(\gamma_A^{(1)} > \gamma_B^{(3)} \mid N_{AS} = n), \tag{3-10}$$

where N_{AS} denotes the active set size of the UE.

Our simulation results of the probability as defined in (3-10) with different effective reuse factors are shown in Fig. 3-5. It can be observed that $Pb(2)$ is ranged between 0.14 and 0.20, and $Pb(3)$ is ranged between 0.62 and 0.70. Hence, we conclude that as the number of soft handover cells (i.e. *n*) increases, the probability that the soft handover scheme will outperform a reuse-3 scheme in average SINR will also be increased.

The average SINR distributions of CEUs with handover list size greater than one are shown in Fig. 3-6 for r_{eff} =1.2, 1.5, and 1.8. It is observed that by using the PFR+SH scheme, the average SINR of the CEUs with handover list size greater than one is increased by approximately 1.8 dB, on average, when comparing with the standard PFR scheme. To link up the results with Table 3-2, we conclude that about 9% (Pb_2+Pb_3) of total users or 26% ((Pb_2+Pb_3)/Pb_E) of CEUs will get SINR improvement by using the PFR+SH scheme, and the relative gain is about 1.8 dB, on average.

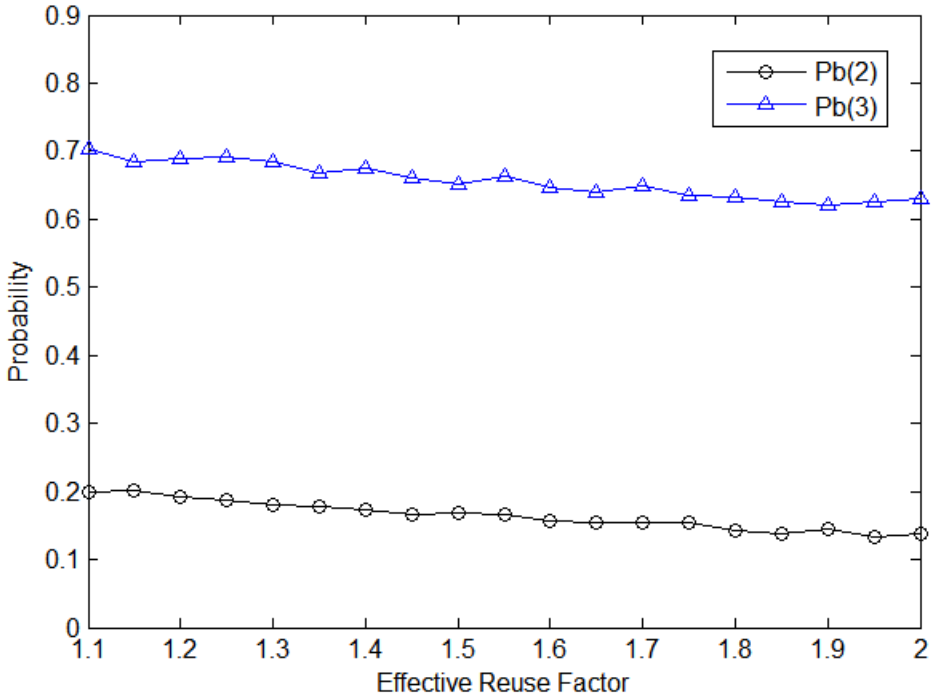

Fig. 3-5 Simulation Results of conditional probability *Pb*(*n*)

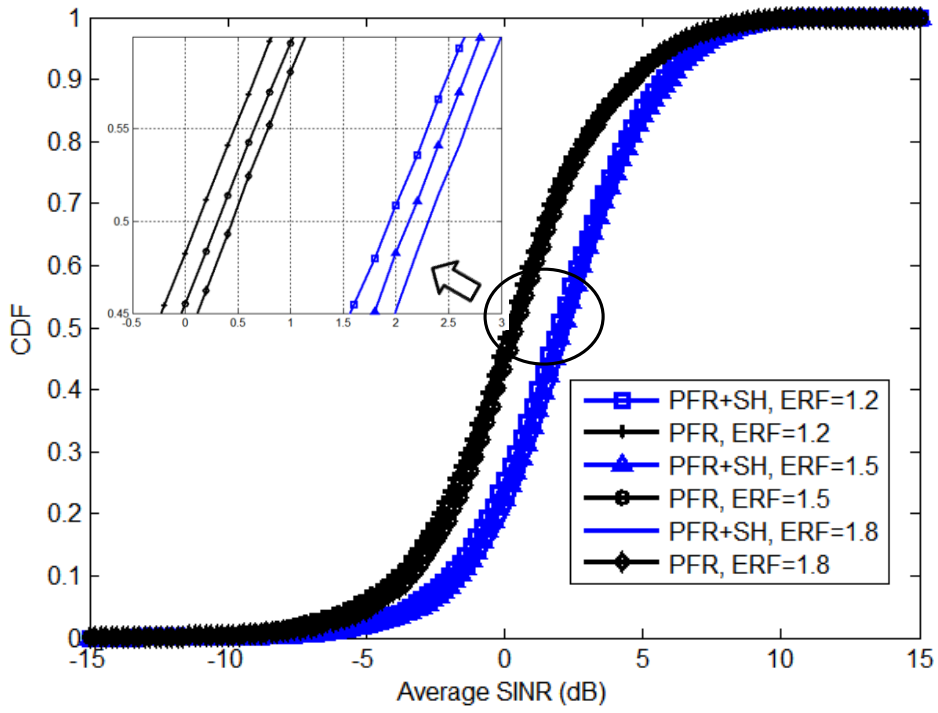

Fig. 3-6 Average SINR distributions of CEUs with handover list size > 1

3.5.3 Link Spectral Efficiency Comparison

A more meaningful metric to look at is the improvement in link spectral efficiency (SE) by accounting for the bandwidth loss effect from the soft handover scheme and the reuse-3 scheme. The condition for this link spectral efficiency improvement can be expressed as

$$\frac{1}{n}\cdot\log_2(1+\gamma_A^{(1)}/\varsigma) > \frac{1}{3}\cdot\log_2(1+\gamma_B^{(3)}/\varsigma), \tag{3-11}$$

where n denotes the number of soft handover cells. It is noted that for a cell edge UE with 2-way or 3-way soft handover, the event $\gamma_A^{(1)} > \gamma_B^{(3)}$ does imply that inequality (3-11) holds and thus leads to link capacity improvement. To capture the link capacity improvement, we further define the *effective link SE* $\tilde{C}_{eff}$ as

$$\tilde{C}_{eff}(\gamma) = \frac{1}{m}\tilde{C}(\gamma), \tag{3-12}$$

where m is a bandwidth loss factor accounting for a reuse-3 scheme (m=3) or a soft handover scheme (m=2 or 3). We note that the loss factor m is set to 1 for the CIUs.

For 3GPP LTE, the link SE at 5 % point of its CDF (i.e. 95% coverage), called 5% user SE, is an important criterion for performance evaluation of different inter-cell interference mitigation schemes [15][44]. Therefore, we adopt this criterion as a performance comparison indicator here. Figure 3-7 demonstrates the effective link SE $\tilde{C}_{eff}$ distributions with r_{eff} =1.2, 1.5, and 1.8; and in particular we focus on the low user SE region. From the figure we observe that the 5% user SE of the PFR+SH scheme is about 1.3 times of that of the standard PFR scheme.

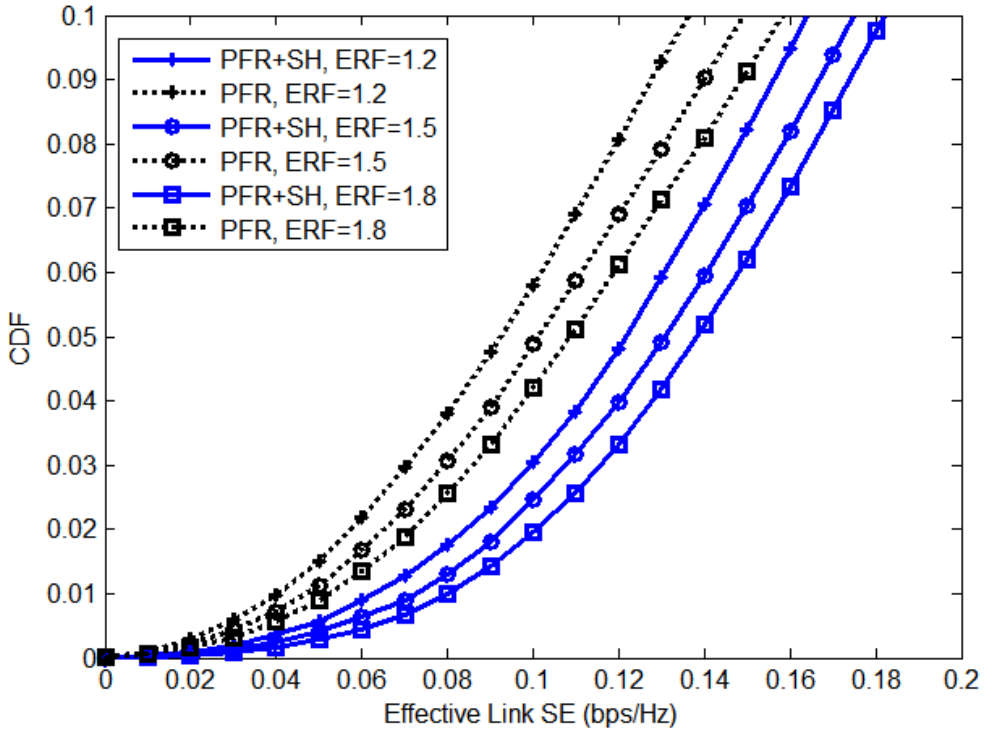

Fig. 3-7 Effective link SE distributions of the standard PFR and the proposed schemes with different effective reuse factors

3.5.4 System Capacity Comparison

Figure 3-8 shows the average cell interior throughput ($T_{Interior}$) and cell edge throughput (T_{Edge}) for the standard PFR scheme and the PFR+SH scheme with different effective reuse factors. From this figure we can have three observations. First, the larger the effective reuse factor is, the smaller the total cell throughput becomes. This is due to the fact that as the effective reuse factor increases, the available bandwidth in each cell is decreased and it results in lower frequency resource utilization. Second, the PFR+SH scheme provides a significant cell edge throughput gain (about 18-92 %) over the PFR scheme, and the gain is more significant when the effective reuse factor is reduced. Third, with the same effective reuse factor, the PFR+SH scheme causes about 11-13 % cell

interior throughput loss as compared with the PFR scheme. This is because in the PFR+SH scheme, the cell center band (F_1) is shared between all CIUs and some CEUs (who are performing soft handover), thus the amount of frequency resource allocated to a CIU, on average, is less than that in the PFR scheme. From the above observations, one can conclude that the PFR+SH scheme is an appropriate method to improve cell edge bit rate and achieve data rate fairness among users.

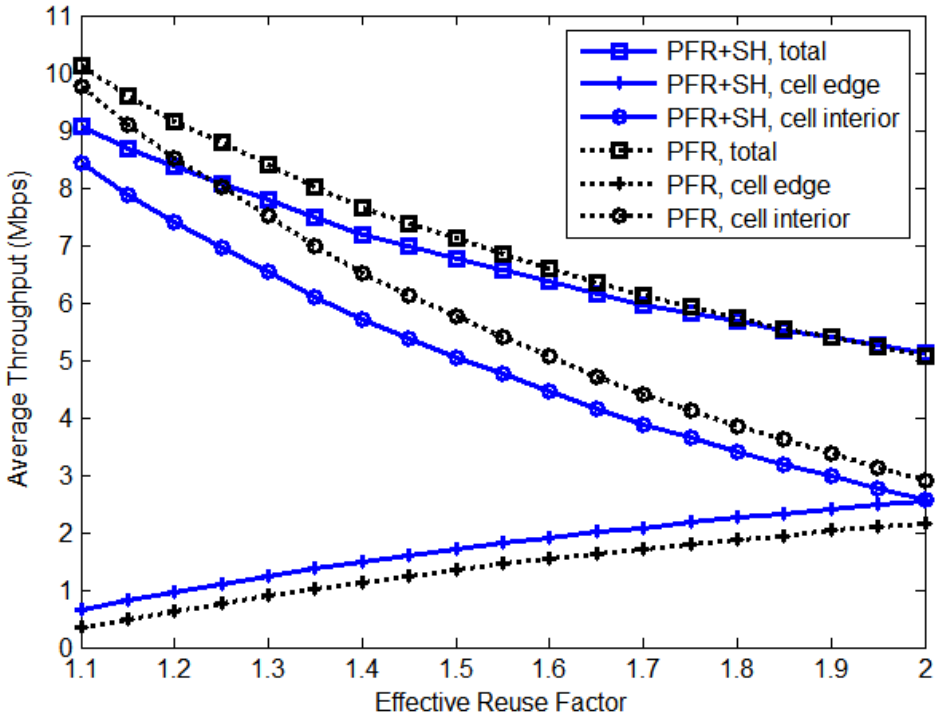

Fig. 3-8 Average throughput performance of the standard PFR and the PFR+SH schemes with different effective reuse factors

We all know that it is very important to consider data rate fairness among users in a mobile communication system. Here, once again, we employ the parameter *f*, which has been brought up in Section 2.5.4 and is defined as the ratio of the average CIU throughput to the average CEU throughput (see (2-21)), to evaluate the *data rate fairness* between

CIUs and CEUs. Note that in the development of 4G mobile communication systems, delivering a more uniform user experience across the cell area is a highly recommendable requirement. In this work, we consider three data rate fairness cases [37]: the first one is f=1, which is called *fair*; the second case is f=2, which is called *less fair*; and the last one is f=3, which is called *least fair*. In the above three cases, the average user throughputs of CEUs are approximately 100%, 50%, and 33.3% of the average user throughputs of CIUs, respectively.

Our simulation results of the average cell throughput at different data rate fairness index f are presented in Fig. 3-9. For comparison, we also show the pure reuse-1 deployment result in the figure. Note that in reuse-1 deployment case the value of f is fixed and is approximately 5.1 from our simulation. As shown in Fig. 3-9, both PFR and PFR+SH schemes outperform reuse-1 assuming f=5.1. This result implies that the influence of accessible bandwidth loss caused by using PFR or PFR+SH scheme can be regained, and it further leads to an improvement in throughput. From Fig. 3-9 one can observe that, as compared with the standard PFR scheme, the PFR+SH scheme can achieve about 8%, 5%, and 3% average cell throughput gains in the *fair*, *less fair*, and *least fair* cases, respectively. The performance improvement can be explained as follows: due to the consideration of the data rate fairness among users, the PFR+SH scheme can distribute the user throughput more evenly to the users than the standard PFR scheme. In other words, the PFR+SH scheme can meet a given data rate fairness index by using a smaller effective reuse factor as compared with the standard PFR scheme. Figure 3-10 shows data rate fairness index f as a function of the effective reuse factors. Take the f=1 case as an example, the corresponding effective reuse factors are 1.83 and 1.68 for the PFR scheme and the PFR+SH scheme, respectively.

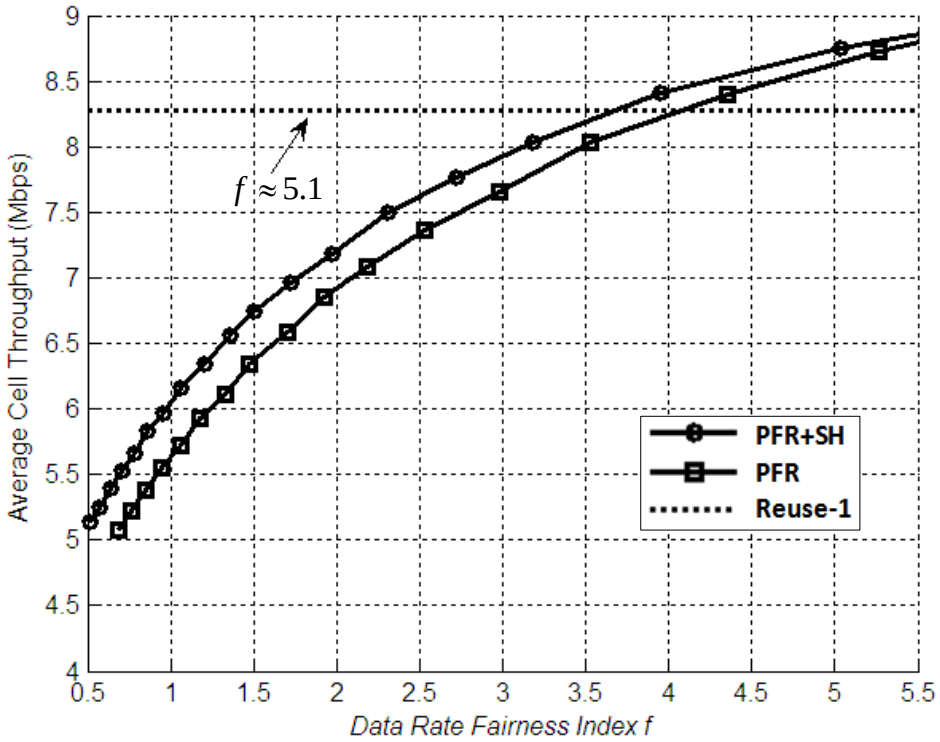

Fig. 3-9 Average throughput performance of the standard PFR and the PFR+SH schemes with different data rate fairness index *f*

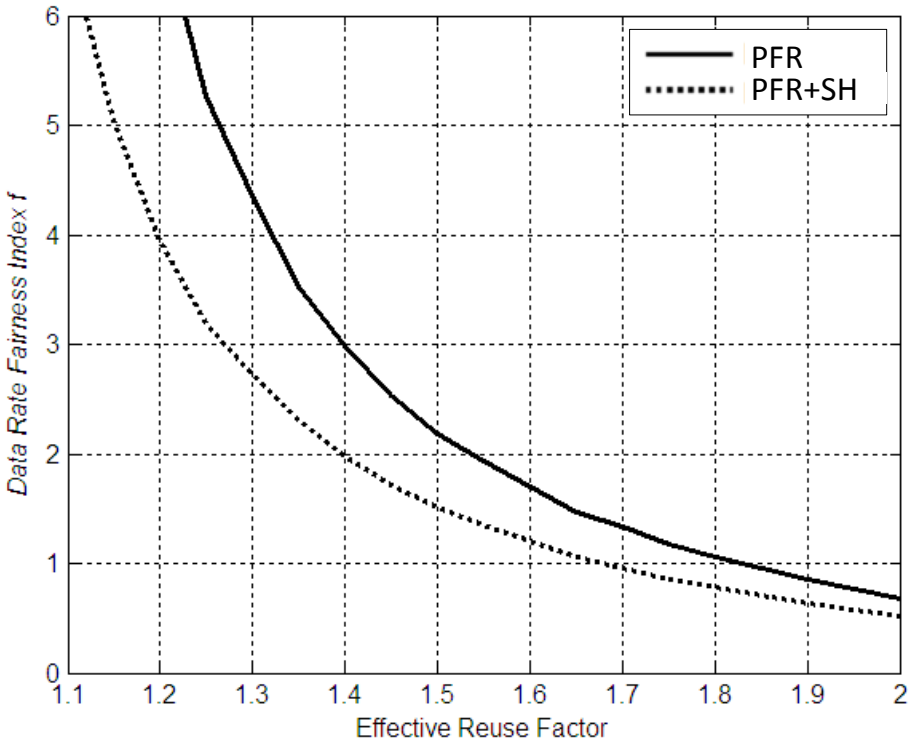

Fig. 3-10 Data rate fairness index *f* as a function of the effective reuse factors

3.6 Summary

Partial frequency reuse is considered one of the most promising ICIC approaches to cope with inter-cell interference problem in OFDMA systems. And, soft handover is currently used as a powerful technique to further improve cell edge performance in 3G CDMA systems. In this chapter, we propose an inter-cell interference mitigation scheme for an OFDMA downlink system, which makes use of both partial frequency reuse and soft handover. The basic idea of the proposed scheme is to dynamically choose between a partial frequency reuse scheme (with a reuse factor of 3) and a soft handover scheme to provide better signal quality for cell edge users. Our simulation results show that compared with standard partial frequency reuse scheme, the proposed scheme helps to improve the link quality and link spectral efficiency of cell edge users. By using our approach, there is a significant cell edge throughput gain over the standard partial frequency reuse scheme and it introduces a relatively low soft handover overhead. Considering data rate fairness among users, the proposed hybrid method also outperforms the standard partial frequency reuse scheme in total cell throughput. Therefore, we conclude that the proposed scheme is a competitive choice to enhance cell edge bit rate and overall system capacity.

Chapter 4 An Inter-Layer Interference Coordination Scheme for Cellular Heterogeneous Networks

4.1 Introduction

By the increasing popularity of connected devices, such as smart phones and tablets, mobile data capacity demand increases faster than spectral efficiency improvement. Recently, a heterogeneous network (commonly referred to as a HetNet) deployment in which low power nodes (LPNs) or small cells overlay within the coverage area of a macro cellular network has been proposed in 3GPP LTE-A as a effective means of expanding mobile network capacity (per unit area) and supporting higher user data rate [15][20]. Overlaying small cells in this way enables higher spectral reuse due to *cell-splitting*.

Two scenarios of co-channel HetNet deployments are discussed in LTE-A:

macro-pico and macro-femto [38]. In the macro-pico case, the small cells are open subscriber group (OSG) cells accessible to all users of the cellular network. In the macro-femto case, the small cells are closed subscriber group (CSG) cells available only to a limited group of users. Although both scenarios are considered in LTE-A, the main focus is the macro-pico scenario. In the subsequent discussions, we consider a basic HetNet deployment scenario with two cell layers, i.e. *macro-layer*[2] and *pico-layer*[2], operating on the same set of frequencies (i.e. co-channel allocation). In brief, a co-channel macro-pico HetNet deployment is assumed.

With large power difference between the two layers and by using the conventional cell selection scheme, the load per picocell may be relatively low in a co-channel macro-pico HetNet. In order to extend the footprint of the picocells and thus increase the offload opportunities from macrocells[3] to picocells, cell range expansion (CRE) technique [23, 24] has recently been introduced in 3GPP LTE-A. It is worthy to note that the CRE technique is not applicable to macro-femto HetNets because of the CSG property of femtocells. The basic idea of CRE is to allow user equipments (UEs) to associate with a picocell even if it is not the strongest cell. Obviously, UEs making use of CRE can experience severe interference conditions since the signal from the associated picocell is weaker than the signals from interfering macrocells. Therefore, in order to ensure robust operation in a co-channel macro-pico HetNet with CRE, the inter-layer (or cross-tier) interference must be effectively addressed.

Due to the large difference in transmit power between the nodes of a HetNet, the inter

[2] Herein, the macro-layer and the pico-layer, respectively, comprise all macrocells and all picocells in the network.

[3] Herein, a macrocell is defined as a high-power node with its antenna typically located above rooftop level (e.g. 32m height).

-layer interference (ILI) is more challenging as compared with the inter-cell interference (ICI) in a cellular macro-only (homogeneous) network. As suggested in [1] and [4], the interference coordination concept could be used not only to deal with the ICI problem in a homogeneous network but also to address the ILI issue in a HetNet. We note that the co-channel macro-pico HetNet with CRE is especially vulnerable to inter-layer interference. For the operation of co-channel macro-pico HetNets with CRE, 3GPP LTE-A (LTE Release 10) includes one new *inter-layer interference coordination* (ILIC) technology based on *time domain* coordinated muting (i.e. TDM) using so-called almost blank subframes (ABS) [21][25]. Nevertheless, the development of ILIC scheme for co-channel macro-pico HetNet with CRE is still an emerging topic for academic research and only a few works have been presented so far. In [52], an interference coordination method based on the divisions of cell border regions was suggested for a macro-pico HetNet, but it did not consider the implementation of CRE. The authors in [22] presented a cooperative scheduling approach based on power coordination to guarantee the signal quality in picocell range expansion area. Here, we refer the readers to [24] for a comprehensive overview of the HetNet deployments with CRE.

In this chapter, we introduce an inter-layer interference coordination scheme on the downlink side for an OFDMA *co-channel macro-pico HetNet* (simply called *macro-pico HetNet* hereafter in this chapter), and in particular we assume that the CRE technique is enabled in the system. The proposed scheme makes use of a combination of power and frequency coordination together with a set of resource allocation rules. The key idea of this scheme is to have a “protected” band for cell-edge pico users on which a reasonable signal quality can be obtained because of the relief of macro interference. We verify the suitability and the degree of performance improvement of the proposed scheme through simulation studies.

The remainder of this chapter is organized as follows. In Section 4.2, we provide the details of picocell range extension concept. In Section 4.3, we illustrate the proposed inter-layer interference coordination scheme. In Section 4.4, we present the system model, measures and assumptions for the performance evaluation. Our simulation results and discussions are given in Section 4.5. Finally, we give conclusions in Section 4.6.

4.2 Picocell Range Expansion

4.2.1 Cell Association Schemes

In a traditional macro-only (homogeneous) network, typically the cell selection (or cell association) is based on the criterion of maximal downlink (average) received signal strength (RSS). In other words, the UE is typically associated to the cell with the strongest downlink RSS (max-RSS) and it can be further expressed as

$$Serving\ \ Cell = \arg\max_{\{i\}} \{RSS_i\}, \tag{4-1}$$

where the index *i* corresponds to the candidate cell index. This cell selection scheme is commonly adopted and identical to the existing cell section scheme used in LTE and WCDMA systems. Note that in this chapter "*RSS*" denotes a long-term average measurement taking into account of transmit power, distance-dependent path loss, shadowing and antenna gain. In practical, RSS can be acquired by observing the power of a received cell-specific reference signal (or pilot signal). In a homogeneous deployment, since all the macrocells typically have similar transmission configurations (such as transmit power level, antenna patterns, etc.) and load conditions, the UE is typically best served by the cell which provides the largest downlink RSS.

However, in the deployments of macro-pico HetNets, under the conventional cell association rule of selecting the cell with the highest downlink received power, the number of UEs associated with picocells is very small. As a consequence, very few UEs benefit from the presence of the picocells and this may further leads to the case where the picocells serve only a few users while at the same time in the macrocells the competition for the available resources would remain high. The limited coverage of picocells is a result of lower transmit power, lower antenna gain and worse propagation conditions compared with macrocells. It is therefore beneficial to have an UE connect to a picocell even if it is not the cell which provides the strongest received power. Generally, such a cell selection scheme is referred as cell range expansion (CRE) of low power nodes.

Very recently, biased-RSS cell selection has been proposed and considered in 3GPP as a promising scheme for realizing CRE of picocells [23][53, 54]. This scheme causes users to select a picocell by adding a cell selection *bias* to the RSS from picocells and it can be given as

$$Serving\ Cell = \arg\max_{\{i\}} \left\{ RSS_i + bias_i \right\}, \tag{4-2}$$

in which the bias*i* (in dB) is chosen to be a positive, non-zero value whenever the candidate cell *i* corresponds to a picocell and is set to zero for all macrocells. Note that the CRE bias values for picocells can have different settings, but they usually have the same setting in a region. As illustrated in Fig. 4-1, such a cell selection strategy would extend the area in which the picocell is selected. In this work, the CRE concept is fulfilled by using biased-RSS cell selection, and we further assume the same CRE bias setting for all picocells in the evaluation system. Unless otherwise stated, the CRE technique spells biased-RSS cell selection scheme in this study.

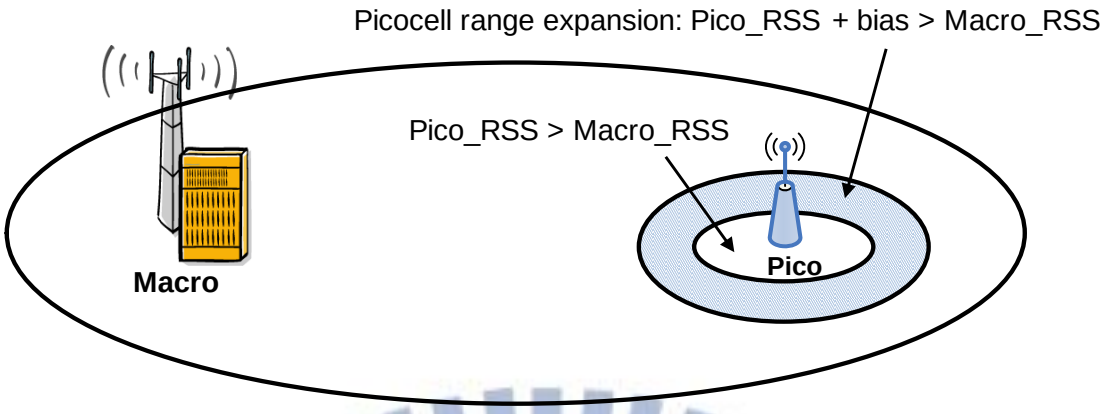

Fig. 4-1 An illustration of picocell range expansion with biased-RSS cell selection

4.2.2 Benefits and Challenges of using CRE

Picocell range expansion may be beneficial in several aspects as follows:

Traffic Offloading: As more and more users are associated to picocells, the loading of those cells will increase while the loading of macrocells will decrease. Obviously, CRE technique potentially provides greater offloading of UEs from the macro-layer onto the pico-layer.

Data rate fairness: To ensure that users remain satisfied, it is very important to deliver a consistent user experience throughout the network. Since CRE technique results in more balance of user distribution between macro-layer and pico-layer, a more uniform user data rate throughput experience across cells (including macrocells and picocells) can be expected.

Uplink Interference: On the uplink, all the UEs have the same maximum transmit power. From uplink point of view, the optimal serving cell choice is determined by the lowest path loss rather than the highest downlink received power. If an UE is associated with the macrocell with the strongest downlink signal (but not with the cell with the minimum path loss), it may cause significant uplink interference to a picocell that is closer

to the UE. With the use of CRE technique, the terminal transmit power, and thus such uplink interference occurrences would be reduced since many more UEs now are able to connect to the picocells that are with lower path loss even if the received signal power from macrocell is significantly higher.

Even so, HetNet deployments using CRE give rise to strong and varied interference conditions across layers. As mentioned above, CRE forces a number of users to connect to picocells even when the picocell is not their strongest serving cell. It should be noted that a large bias value will result in a low experienced SINR (signal to interference plus noise power ratio) values for UEs connected to picocells; and further, it increases the risks of introducing higher user outage rate (in terms of user SINR) problems in the system. As a consequence, inter-layer interference management is critical in order to ensure robust communications in a macro-pico HetNet that realizes picocell range extension.

4.3 Proposed Inter-Layer Interference Coordination Scheme

Considering a macro-pico HetNet, inter-layer interference could be strong and varied significantly when the increased LPN footprint (i.e. CRE) technique is utilized. To overcome the interference issue, the picocell needs to perform interference coordination with the dominant macro interferers. In the following, the proposed inter-layer interference coordination (ILIC) scheme that applies restrictions to the frequency and power resources in a coordinated way between macro and pico cell layers is described. Herein, we call this method the *PF-ILIC* scheme.

For the rest of this chapter, we use the following abbreviations for simplicity: Any UE served by the macrocell is referred to as a "*MUE*". The term "*PUE*" refers to a UE which is connected to a picocell. Furthermore, the term "*range expansion PUE*" (simply called *RE-PUE* hereafter) refers to any PUE that is additionally served by a picocell due to CRE.

More specifically, the RE-PUEs are those UEs who are originally attached to macrocells, but now are served by picocells via the utilization of CRE.

The PF-ILIC scheme consists of three key components; they are frequency-power arrangement, band scheduling, and adaptive frequency partition.

4.3.1 Frequency-Power Arrangement

A typical interference-limited case when adopting CRE is that a noticeable fraction of cell-edge PUEs will suffer from macrocell interference. In order to make those PUEs work properly, it is fairly reasonable that one part of the frequency resources is reserved for cell-edge PUEs, on which the corresponding transmission power of the macrocells (or macro-layer) is reduced. Figure 4-2 shows the frequency-power arrangement of the PF-ILIC method. As depicted in Fig. 4-2, the available spectrum is divided into two distinct subbands in every cell. One subband is named *normal band* (*NB*) and the other subband is termed as *platinum band* (*PB*). Let P_t^{macro} and P_t^{pico} be the maximum transmission power level (or power spectrum density) for macrocell and picocell, respectively, and they can be given as

$$P_t^{node} = \frac{P_T^{node}}{BW_{all}}, \ (node \in \{macro, pico\}) \tag{4-3}$$

where P_T^{node} denotes the total transmission power of the node and BW_{all} is the total available bandwidth. Note that in (4-3), the superscript *node* stands for a macrocell or a picocell. For each picocell, both normal band and platinum band are transmitted with maximum power level. That is, a flat transmission power spectrum is applied on the whole bandwidth of picocells. However, for each macrocell, only the normal band has maximum transmission power level while the platinum band is restricted in power. Herein, we further

assume that the power is equally spread on the normal/platinum bands individually in macrocells. In such arrangement, we can have "*protected band*" (i.e. platinum band) for PUEs on which the significant interference from macrocells is alleviated.

Referring to Fig. 4-2, a parameter η, called *power reduction factor*, is introduced to represent the power ratio of normal band to platinum band. This factor is chosen to be a value greater than one for macrocells while it equals one for picocells. In this work, the power reduction factor (η) corresponding to macrocells is set to 10 dB for the proposed method [29][55]. In other words, the transmission power on platinum band for each macrocell is 10 times less than that on normal band.

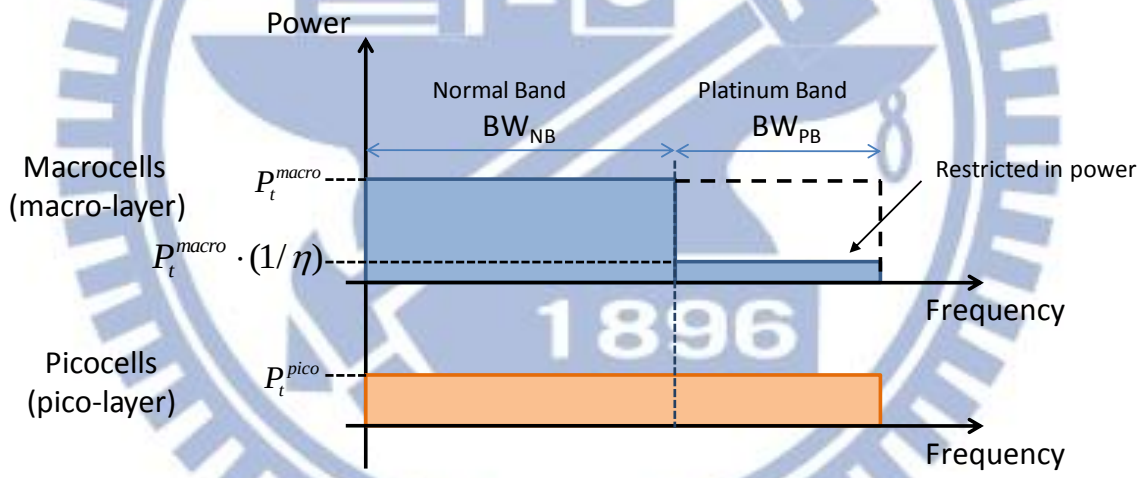

Fig. 4-2 The proposed frequency-power arrangement for co-channel macro-pico HetNet

4.3.2 Band Scheduling Rules

In order to take advantage of extending picocell coverage, the dominant interference from macrocells must be effectively addressed. With the proposed frequency-power arrangement, it is useful for picocells to serve the UEs at cell borders by using platinum

band since the interference is significant lower due to the power reduction at macrocells. Therefore, in the PF-ILIC scheme, the picocell primarily schedules cell-edge users to use the platinum band, whereas the users closer to the picocell (i.e. cell-interior users) have exclusive access to the normal band and nevertheless, they may be granted with the frequency resources of platinum band if it is not taken by the cell-edge users. Considering the macrocells, it is better to *only* serve central users (i.e. cell-interior users) on the platinum band since they are more insensitive to power reduction. By doing this, the frequency resources on platinum band could be effective utilized in macrocells. On the other hand, the normal band in macrocells can be applied to all the users, including edge and central users. We note that cell central users in a macrocell are allowed to access *both* platinum band and normal band since the inferior frequency resources (i.e., platinum band) might not be enough to supply these users and hence it would further lead to a loss on overall system capacity.

The proposed band scheduling method work together with the split of users into cell-interior users (CIUs) which have low probability to be interfered by neighbor cells and cell-edge users (CEUs) which have high probability to be interfered by neighbor cells. Note that for all types of ICIC schemes applied in homogeneous networks it is also essential to distinguish between cell-interior users and cell-edge users. In this chapter, once again, the widely accepted approach, G-factor based method (see Section 3.3.1), is employed to classify UEs into CIUs and CEUs. Recall that the G-factor is the *wideband average SINR* measured by an UE in a fully-loaded network with universal frequency reuse and uniform power allocation. In the proposed method, the G-factor can be obtained from measuring reference signals (or pilot signals) over the normal band. Herein, an UE is regarded as a cell-edge user if the G-factor measured at the UE is smaller than a threshold of 0 dB [26][30][50]; otherwise, the UE is treated as a cell-interior user.

Assuming a fully loaded system, it becomes unlikely that cell-interior PUEs would be able to access the platinum band, and they would thus be confined to the normal band. This causes a separation of user groups for which the cell-interior PUEs occupy the normal band only while the cell-edge PUEs use the platinum band. As a result, in the case of a fully loaded system, the proposed band scheduling method can be summarized in Table 4-1.

Table 4-1 The proposed band scheduling method under a fully loaded system

	Macrocell	Picocell
Normal Band	CIUs and CEUs	CIUs
Platinum Band	CIUs	CEUs

4.3.3 Adaptive Frequency Partitioning

Herein, we introduce the frequency partition ratio (μ) of the PF-ILIC scheme as

$$\mu \equiv \frac{BW_{PB}}{BW_{all}} = \frac{BW_{PB}}{BW_{NB} + BW_{PB}} \ (<1), \tag{4-4}$$

where BW_{PB} and BW_{NB} are the configured bandwidth of platinum band and normal band, respectively. Recall that the main purpose for us to have a platinum band is to create protected zone for PUEs who have a low geometry factor (G-factor), and this is especially important for RE-PUEs. With the user grouping threshold of 0 dB, a PUE will always be treated as a cell-edge PUE if its received signal power from the macrocell is higher than that of serving picocell. That is to say, a RE-PUE will always be a cell-edge PUE in the evaluation system. As a rule of thumb, it can be assumed that the amount of protected frequency resources should be approximately proportional to the number of cell-edge PUEs which have to operate at a low SINR. Accordingly, we set the frequency partition

ratio (μ) as the ratio of the number of cell-edge PUEs to the number of total users (including PUEs and MUEs), and it can be expressed by

$$\mu = \frac{N_{cell\text{-}edge\ PUEs}}{N_{total\ UEs}}, \tag{4-5}$$

where $N_{cell\text{-}edge\ PUEs}$ and $N_{total\ UEs}$ denote the number of cell-edge PUEs and total users, respectively. The frequency partition ratio (μ) can be adaptively configured according to the cell-edge PUEs' distribution in the system.

4.4 System Model, Measures and Assumptions

4.4.1 Reference System Descriptions and Heterogeneous Network Layout

For comparison, we consider a reference system, i.e. the macro-pico HetNet with conventional reuse one (reuse-1) scheme, in which no inter-layer interference mitigation scheme between macro-layer and pico-layer is performed. All macrocells and picocells transmit with its maximum power level over the entire bandwidth. In addition, there is no resource allocation restriction applied to different user groups (i.e. CIUs and CEUs) in each cell. Figure 4-3 shows the related frequency-power setting of the reference system.

The considered system model of macro-pico HetNet in a tri-sector cellular layout is illustrated in Fig. 4-4. As shown in the figure, each cell site (base station) controls three 120-degree sectors (macrocells) and two picocells are evenly placed in each sector (macrocell) at a distance of (2/3)r from base station, where r is the macrocell radius. Herein, the terms macrocell and sector are interchangeable. Note that this cellular system configuration of two LPNs within each macro geographical area is also used in 3GPP for HetNet performance evaluations [56, 57].

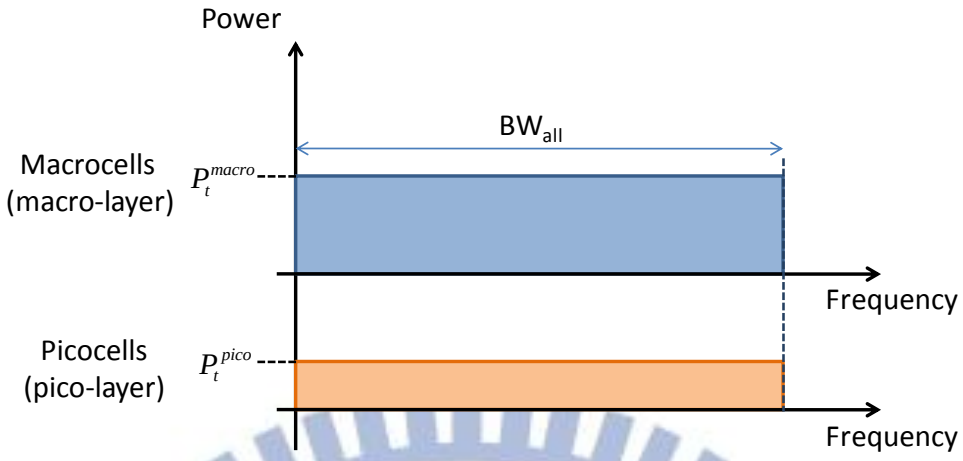

Fig. 4-3 Frequency-power setting of the HetNet reference system

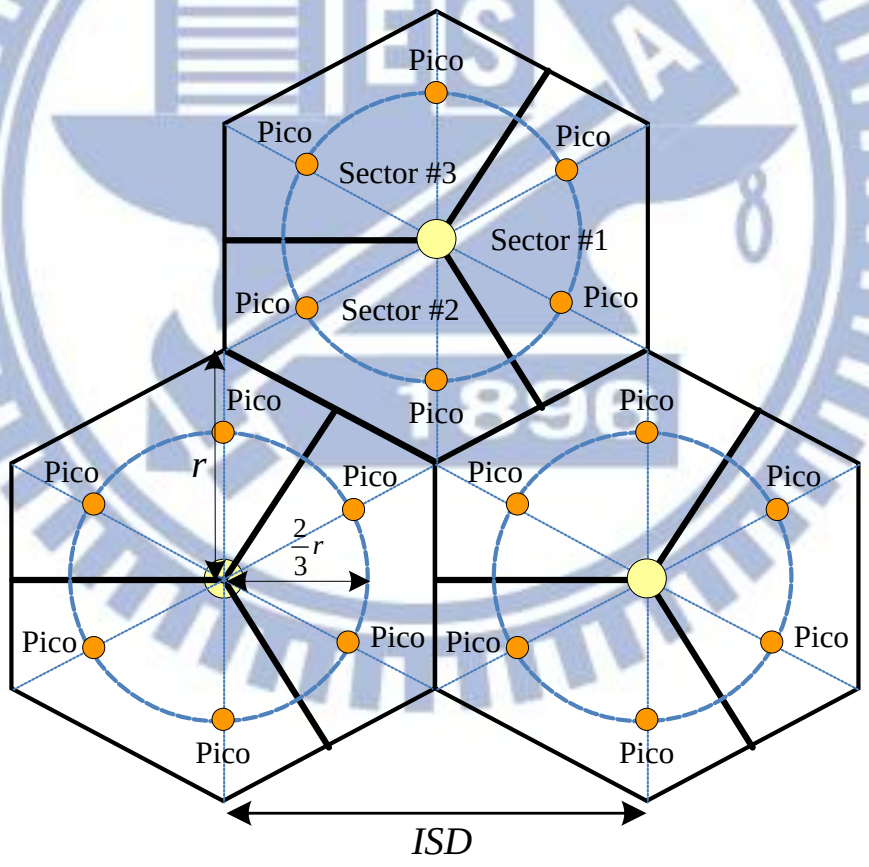

Fig. 4-4 The macro-pico HetNet layout of the evaluation system

4.4.2 Average SINR Modeling

In this work, we do not consider fast fading and assume radio link is subject to propagation loss and log-normally distributed shadowing. Note that no fast fading modeling is considered in 3GPP for HetNet performance evaluation [15]. To start with, we consider the average SINR for a MUE on the normal band and it can be expressed as

$$\gamma_{I,NB}^{MUE} = \gamma_{E,NB}^{MUE} = \frac{P_t^{macro} \cdot A_s \cdot L_s \cdot S_s}{\sum_{i \in \{\Phi_{macro} - s\}} P_t^{macro} \cdot A_i \cdot L_i \cdot S_i + \sum_{j \in \Phi_{pico}} P_t^{pico} \cdot A_j \cdot L_j \cdot S_j + P_N}, \quad (4\text{-}6)$$

where A_k, L_k and S_k are the antenna gain, path loss and shadow fading loss from the cell k to the MUE, respectively; the subscripts I and E stand for the CIUs and CEUs, respectively; the subscripts s, i and j stand for the serving cell, the interfering macrocells and the interfering picocells, respectively; Φ_{macro} and Φ_{pico} are the sets of macrocells and picocells, respectively; P_N denotes the received noise power spectrum density. We recall that in the proposed method, the normal band is available to all MUEs, including cell-interior and cell-edge MUEs.

Next, considering a cell-interior MUE on the platinum band, its average SINR can be written as

$$\gamma_{I,PB}^{MUE} = \frac{P_t^{macro} \cdot (1/\eta) \cdot A_s \cdot L_s \cdot S_s}{\sum_{i \in \{\Phi_{macro} - s\}} P_t^{macro} \cdot (1/\eta) \cdot A_i \cdot L_i \cdot S_i + \sum_{j \in \Phi_{pico}} P_t^{pico} \cdot A_j \cdot L_j \cdot S_j + P_N}. \quad (4\text{-}7)$$

We remind that η is the power reduction factor and also note that according to our band scheduling method, only cell-interior MUEs are qualified to use the platinum band. Similarly, the average SINR for a cell-interior PUE on the normal band and a cell-edge PUE on the platinum band are given by (4-8) and (4-9), respectively.

$$\gamma_{I,NB}^{PUE} = \frac{P_t^{pico} \cdot A_s \cdot L_s \cdot S_s}{\sum_{i \in \Phi_{macro}} P_t^{macro} \cdot A_i \cdot L_i \cdot S_i + \sum_{j \in \{\Phi_{pico} - s\}} P_t^{pico} \cdot A_j \cdot L_j \cdot S_j + P_N} \quad (4\text{-}8)$$

$$\gamma_{E,PB}^{PUE} = \frac{P_t^{pico} \cdot A_s \cdot L_s \cdot S_s}{\sum_{i \in \Phi_{macro}} P_t^{macro} \cdot (1/\eta) \cdot A_i \cdot L_i \cdot S_i + \sum_{j \in \{\Phi_{pico} - s\}} P_t^{pico} \cdot A_j \cdot L_j \cdot S_j + P_N} \quad (4\text{-}9)$$

Regarding the calculations for the reference system, let $\hat{\gamma}_I^{MUE}$ and $\hat{\gamma}_E^{MUE}$ denote that average SINR of a cell-interior MUE and a cell-edge MUE, respectively. Obviously, one can obtain $\hat{\gamma}_I^{MUE} = \hat{\gamma}_E^{MUE} = \gamma_{I,NB}^{MUE} = \gamma_{E,NB}^{MUE}$. Moreover, let $\hat{\gamma}_I^{PUE}$ and $\hat{\gamma}_E^{PUE}$ be the average SINR of a cell-interior PUE and a cell-edge PUE in the reference system, respectively. Then we have $\hat{\gamma}_I^{PUE} = \hat{\gamma}_E^{PUE} = \gamma_{I,NB}^{PUE}$.

4.4.3 Link Spectral Efficiency Estimation

The maximum theoretical data rate with single antenna transmission in static channel can be derived using the Shannon formula [41]. However, the Shannon capacity bound cannot be reached in practice due to some implementation issues. To evaluate the achievable throughput as a function of the average received SINR while using AMC (adaptive modulation and coding), a modified form of the Shannon bound was proposed in a 3GPP technical report [58] to calculate link capacity in an LTE system, and it is given by

$$\hat{C}(\gamma) = \begin{cases} 0 & : \text{for } \gamma \le \gamma_{\min} \\ \xi \cdot S(\gamma) & : \text{for } \gamma_{\min} < \gamma < \gamma_{\max}, \text{ (bps/Hz)} \\ C_{\max} & : \text{for } \gamma \ge \gamma_{\max} \end{cases} \quad (4\text{-}10)$$

in which γ denotes the given SINR and ξ is the attenuation factor applied to the Shannon bound given by $S(\gamma) = \log_2(1+\gamma)$ which achieves C_{max} at $\gamma_{\max}$ or beyond and

0 at $\gamma_{\min}$ or lower. The equation imposes an upper limit of 4.8 (bps/Hz) (C_{max}) of spectral efficiency according to the hard spectral efficiency given by modulation and coding scheme (MCS). Moreover, it was shown in [58] that (4-10) with $\xi = 0.75$ yields an excellent match to the link capacity performance of 3GPP LTE over the range of SINR which it operates; and further, the maximum SINR ($\gamma_{\max}$) and minimum SINR ($\gamma_{\min}$) values of the corresponding operation range obtained from simulation are approximately 17 dB and -6.5 dB, respectively. In this work, we employ this modified form of the Shannon bound with the above recommended values to evaluate the link spectral efficiency.

4.4.4 Throughput Calculation

We assume that the users are uniformly distributed within cell coverage and that each user has unlimited traffic to transmit on the downlink and hence all frequency resources designated for each cell are fully utilized (a fully loaded system). Under a fair scheduler (equal resource sharing between users), the system capacity *T* can be calculated as [42, 43]

$$T = BW \cdot \nu \cdot \int \hat{C}(\gamma) f_{\gamma}(\gamma) d\gamma, \tag{4-11}$$

where ν is a loss factor that accounts for the system overhead, $f_{\gamma}(\gamma)$ is the probability density function of SINR γ, and *BW* denotes the allocated bandwidth. In this work, $\nu = 1$ is assumed.

Considering the HetNet with PF-ILIC scheme, we assume that a fair scheduler is applied to normal/platinum bands. From (4-11), the average cell-interior throughput and cell-edge throughput of a macrocell can be written as (4-12) and (4-13), respectively,

$$T_{Interior}^{macro} = BW_{NB} \cdot \left(\frac{Pb_I^{MUE}}{Pb_I^{MUE} + Pb_E^{MUE}}\right) \int \hat{C}(\gamma_{I,NB}^{MUE}) f_{\gamma_{I,NB}^{MUE}}(\gamma_{I,NB}^{MUE}) d\gamma_{I,NB}^{MUE} + BW_{PB} \int \hat{C}(\gamma_{I,PB}^{MUE}) f_{\gamma_{I,PB}^{MUE}}(\gamma_{I,PB}^{MUE}) d\gamma_{I,PB}^{MUE}, \quad (4\text{-}12)$$

$$T_{Edge}^{macro} = BW_{NB} \cdot \left(\frac{Pb_E^{MUE}}{Pb_I^{MUE} + Pb_E^{MUE}}\right) \int \hat{C}(\gamma_{E,NB}^{MUE}) f_{\gamma_{E,NB}^{MUE}}(\gamma_{E,NB}^{MUE}) d\gamma_{E,NB}^{MUE}, \quad (4\text{-}13)$$

in which Pb_I^{MUE} and Pb_E^{MUE} are the (statistically) probabilities of cell-interior MUEs and cell-edge MUEs, respectively (ratio of cell-interior/cell-edge MUEs to total users in number). Note that in (4-12), the first term and second term that appears on the right hand side represent the cell-interior throughput that contribute from normal band and platinum band, respectively (refer to Table 4-1). Furthermore, the average cell-interior throughput and cell-edge throughput of a picocell can be given by (4-14) and (4-15), respectively.

$$T_{Interior}^{pico} = BW_{NB} \cdot \int \hat{C}(\gamma_{I,NB}^{PUE}) f_{\gamma_{I,NB}^{PUE}}(\gamma_{I,NB}^{PUE}) d\gamma_{I,NB}^{PUE} \quad (4\text{-}14)$$

$$T_{Edge}^{pico} = BW_{PB} \cdot \int \hat{C}(\gamma_{E,PB}^{PUE}) f_{\gamma_{E,PB}^{PUE}}(\gamma_{E,PB}^{PUE}) d\gamma_{E,PB}^{PUE} \quad (4\text{-}15)$$

With regard to the reference system, by adopting a fair scheduler, the average cell-interior throughput and cell-edge throughput of a macrocell and that of a picocell can be, respectively, obtained by (4-16), (4-17), (4-18), and (4-19),

$$T_{Interior}^{macro} = BW_{all} \cdot \left(\frac{Pb_I^{MUE}}{Pb_I^{MUE} + Pb_E^{MUE}}\right) \int \hat{C}(\hat{\gamma}_I^{MUE}) f_{\hat{\gamma}_I^{MUE}}(\hat{\gamma}_I^{MUE}) d\hat{\gamma}_I^{MUE}, \quad (4\text{-}16)$$

$$T_{Edge}^{macro} = BW_{all} \cdot \left(\frac{Pb_E^{MUE}}{Pb_I^{MUE} + Pb_E^{MUE}}\right) \int \hat{C}(\hat{\gamma}_E^{MUE}) f_{\hat{\gamma}_E^{MUE}}(\hat{\gamma}_E^{MUE}) d\hat{\gamma}_E^{MUE}, \quad (4\text{-}17)$$

$$T_{Interior}^{pico} = BW_{all} \cdot \left(\frac{Pb_I^{PUE}}{Pb_I^{PUE} + Pb_E^{PUE}}\right) \int \hat{C}(\hat{\gamma}_I^{PUE}) f_{\hat{\gamma}_I^{PUE}}(\hat{\gamma}_I^{PUE}) d\hat{\gamma}_I^{PUE}, \quad (4\text{-}18)$$

$$T_{Edge}^{pico} = BW_{all} \cdot (\frac{Pb_E^{PUE}}{Pb_I^{PUE} + Pb_E^{PUE}}) \int \hat{C}(\hat{\gamma}_E^{PUE}) f_{\hat{\gamma}_E^{PUE}}(\hat{\gamma}_E^{PUE}) d\hat{\gamma}_E^{PUE}, \quad (4\text{-}19)$$

in which Pb_I^{PUE} and Pb_E^{PUE} are the (statistically) probabilities of cell-interior PUEs and cell-edge PUEs, respectively. Note that the setting of frequency partition ratio (μ) in the PF-ILIC scheme could be chosen according to the statistical results of Pb_E^{PUE}.

After having the average throughput of the cell interior users and cell edge users, the average (total) macrocell/picocell throughput thus can be calculated as

$$T_{Cell}^{macro/pico} = T_{Interior}^{macro/pico} + T_{Edge}^{macro/pico}. \quad (4\text{-}20)$$

Then, the metric of average *macrocell area throughput* is introduced here to evaluate the system throughput per single-macrocell coverage area [59], and it is described as

$$T^{area} = T_{Cell}^{macro} + N_p \cdot T_{Cell}^{pico}, \quad (4\text{-}21)$$

where N_p denotes the number of picocells within each macro geographical area. Note that the value of N_p equals 2 in the simulation system (see Fig. 4-4).

4.4.5 Simulation Method and Simulation Parameters

Static snapshot simulations have been used. The average SINR distribution (i.e. $f_\gamma(\gamma)$) is obtained through Monte Carlo simulations involving 2000 random placement of users geographically. Simulation assumptions and parameters basically follow the 3GPP evaluation criteria for HetNet [15]. The available downlink system bandwidth is fixed at 10 MHz. The simulated network layout assumes a hexagonal grid with 19 cell sites and a cell site has three sectors. In addition, there are two circular picocells deployed in each

macrocell with fixed positions (see Fig. 4-4). For the underlying macro scenario, 3GPP macro *Case 1* (i.e. inter-site distance (ISD) of 500 meters) is used. Moreover, we assume that the macrocell uses the 3D directional antenna pattern (including horizontal pattern and vertical pattern) [15] and the picocell adopts omni-directional antenna. A distance-dependent path loss with a propagation loss exponent of 3.76 and a lognormal shadowing with a standard deviation of 8 (10) dB for the macrocells (picocells) are assumed. Note that the path loss model from macrocell to UE and that from picocell to UE are different. Table 4-2 summarizes the main simulation parameters.

Table 4-2 Simulation parameters and assumptions

Parameters	Macro	Pico
Cellular layout	19 cell sites, 3 sectors per site	2 pico cells per sector
Minimum distance	35m (between UE and cell site)	10m (between UE and pico)
Distance-dependent path loss	$128.1+37.6\log_{10}(R)$, R in km	$140.7+37.6\log_{10}(R)$, R in km
Shadowing standard deviation	8 dB	10 dB
Shadowing correlation	0.5 (between cell site) 1 (between sectors)	0.5
Antenna pattern	3D antenna as described in [15]	Omi-directional (horizontal)
Total Tx power	46 dBm	30 dBm
Antenna gain	14 dBi	5 dBi
Inter-site distance (ISD)	500 m	
Carrier frequency	2 GHz	
System bandwidth	10 MHz	
UE antenna gain	0 dBi	
UE noise figure	9 dB	
Penetration loss	20 dB	
Macrocell/UE antenna height	32 m/1.5 m	
Correlation distance of shadowing	50 m	

4.5 Numerical Results and Discussions

Our computer simulations are conducted for the macro-pico HetNet with conventional reuse-1 scheme and the macro-pico HetNet with the PF-ILIC scheme. Furthermore, we consider the CRE bias value ranged between 0 and 16 dB. Note that the case of CRE bias=0 dB refers to the system without applying the CRE technique.

4.5.1 User Association Statistics

To begin with, we plot in Fig. 4-5 the cell association statistics as a function of the CRE bias, and in order to provide further information on the effect of the CRE technique, the fractions of cell-interior/cell-edge PUEs (Pb_I^{PUE} and Pb_E^{PUE}), cell-interior/cell-edge MUEs (Pb_I^{MUE} and P_E^{MUE}), and RE-PUEs are also presented in the figure. One can see that under the cell selection algorithm of selecting the cell with the highest downlink RSS (i.e. without CRE), the number of UEs associated with picocells is small. As shown in Fig. 4-5, observing the case of CRE bias=0dB, only 13% of UEs are associated with picocells, whereas 87% of UEs are still connected to macrocells. On the other hand, one can find that as the CRE bias value is increased, there are more UEs being attached to picocells. For example, considering the case that the CRE bias is equal to 8 dB, it is observed that 31% of UEs are now connected to picocells, and thus the corresponding percentage value for MUEs is reduced to 69%. It is clearly observed how the offload from macrocells to picocells is increased while applying the CRE technique. This is due to the fact that as the CRE bias increases, the number of MUEs which are now become RE-PUEs increases; and further, we notice from the figure that compared with the cell-interior MUEs, the cell-edge MUEs are more likely to be attracted by picocells. Besides, since RE-PUEs are treated as

cell-edge PUEs, the percentage of cell-interior PUEs remains unchanged with different CRE bias values, as shown in Fig. 4-5. Moreover, one can observe from Fig. 4-5 that the frequency partition ratio (μ) in the proposed scheme is adapted to the CRE bias value. Recall that in the PF-ILIC scheme, the frequency partition ratio (μ) equals to the percentage of cell-edge PUEs. For instance, assuming CRE bias=8 dB, the frequency partition ratio could be set to 0.22 when implementing the PF-ILIC scheme.

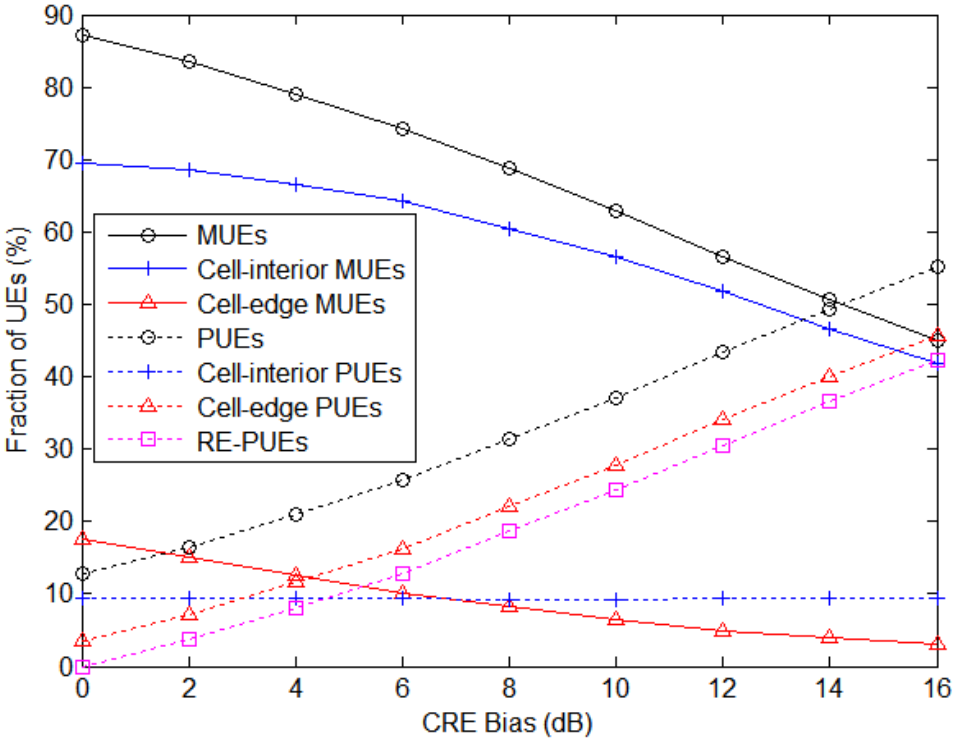

Fig. 4-5 User association statistics of the evaluated HetNet system under various CRE bias values

4.5.2 Link Quality Analysis

Although the CRE technique can further improve load balance between macro-layer and pico-layer, it generates RE-PUEs which are significantly interfered by the macrocells. Therefore, when we consider a macro-pico HetNet with CRE, it is important to examine the link quality of the RE-PUEs, i.e. the extremely-low SINR users. The average SINR CDFs (cumulative distributed functions) of RE-PUEs are plotted in Fig. 4-6 for CRE bias=4, 8, and 12 dB. Note that as shown in Fig. 4-5, the percentages of RE-PUEs in the cases of bias=4, 8, and 12 dB are, respectively, around 8%, 19%, and 31% in the evaluation system. One can observe from Fig. 4-6 that as compared with the conventional reuse-1 scheme, the PF-ILIC scheme yields a significant improvement in average SINR of the RE-PUEs. For example, observing the 50%-tile of SINR CDFs in Fig. 4-6, the PF-ILIC scheme improves over the reuse-1 scheme by approximately 8 dB. This is because in the PF-ILIC scheme, the RE-PUEs will operate on the “protected band”, i.e. the platinum band, on which the macrocell interference is reduced significantly.

As a metric of network performance evaluation, the service outage probability is referred as the fraction of UEs for which the average SINR falls below the SINR threshold for the receiver to function appropriately. According to (4-10), the corresponding SINR threshold is set to -6.5 dB in this study. Note that in LTE systems, the range of average SINR threshold for correctly decoding the control channels is between -6 and -7 dB [14][60]. Figure 4-7 illustrates the service outage probability with different CRE bias values. As expected, the PF-ILIC scheme gives much better results as compared with the conventional reuse-1 scheme. To exemplify this, using a CRE bias value of 8 dB would lead to nearly 10% of the users in the reuse-1 system experiencing coverage problems; however, the corresponding value is just about 0 in the PF-ILIC case. Moreover,

considering the practical system deployment criterion of 5% outage probability [14], one can see from Fig. 4-7 that the CRE bias values less than about 6 dB are feasible in the reuse-1 system while the bias values up to approximately 15 dB can be tolerated for the system with the PF-ILIC scheme. From the above observations, we can conclude that the PF-ILIC scheme is an appropriate method to carry out the CRE concept even if a large CRE bias value is used.

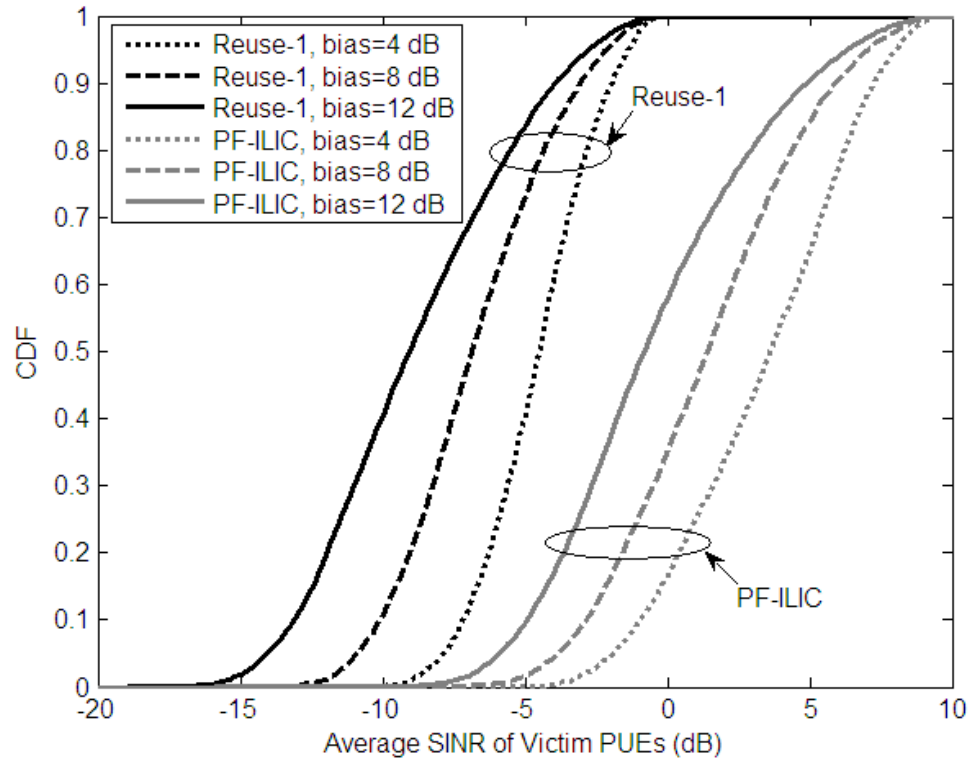

Fig. 4-6 Average SINR distributions of RE-PUEs under different CRE bias values

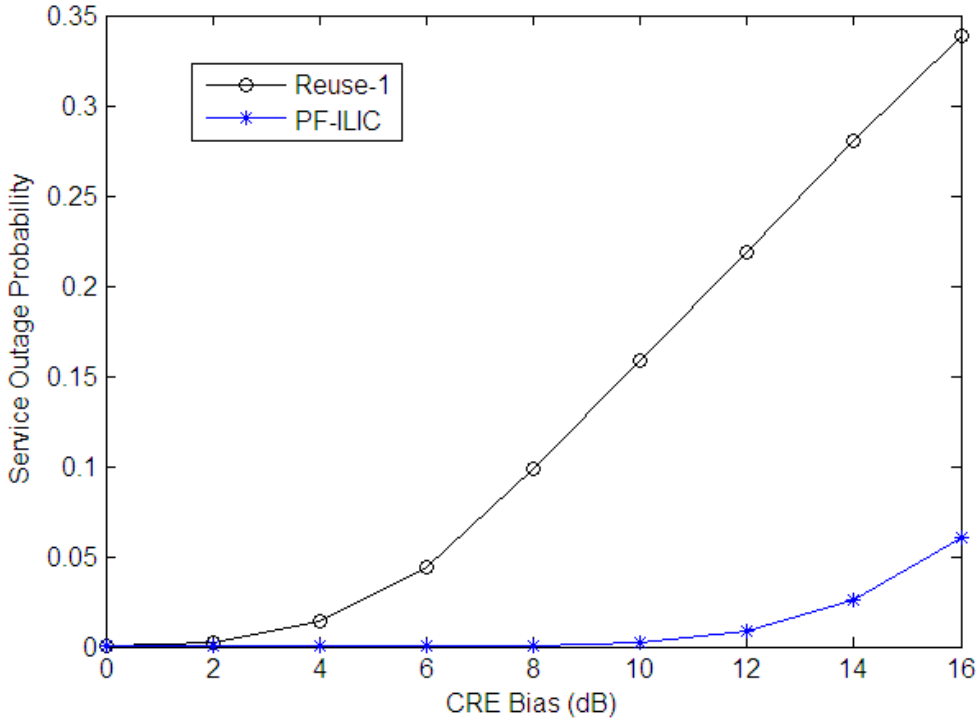

Fig. 4-7 Service outage rate with different CRE bias values

4.5.3 Throughput Performance Analysis

Figure 4-8 shows the average macrocell throughput (T_{Cell}^{macro}), picocell throughput (T_{Cell}^{pico}) and macrocell area throughput (T^{area}) for the conventional reuse-1 scheme and the PF-ILIC scheme with different CRE bias values. Recall that the single-macrocell coverage area contains one macrocell and two picocells. From the figure, we have three observations. First, the PF-ILIC scheme provides a significant picocell throughput gain over the reuse-1 scheme and the gain is increased as the CRE bias increases. More specifically, approximately 100% and 200% average picocell throughput gain can be found at CRE bias of 6 dB and 12dB, respectively. This is reasonable since the number of service outage users can be greatly reduced through using the PF-ILIC scheme. As a fair scheduler is assumed

in this study, the picocell throughput loss turns out to be proportional to the number of service outage users in the system. Second, the PF-ILIC scheme causes about 2-7% macrocell throughput loss as compared with the reuse-1 scheme. This is because in the proposed PF-ILIC scheme, the platinum band in each macrocell is used with reduced power (by 10 dB in this work), which favors PUEs while harms MUEs. Third, compared with the reuses-1 scheme, the PF-ILIC scheme improves the macrocell area throughput by 25-55%, and we further notice that the improvement becomes prominent when the CRE bias is getting larger. This shows that the decreased macrocell throughput caused by employing the PF-ILIC scheme can be regained from the greatly increased picocell throughput, and it turns out to be a considerable macrocell area throughput gain (i.e. total system capacity gain).

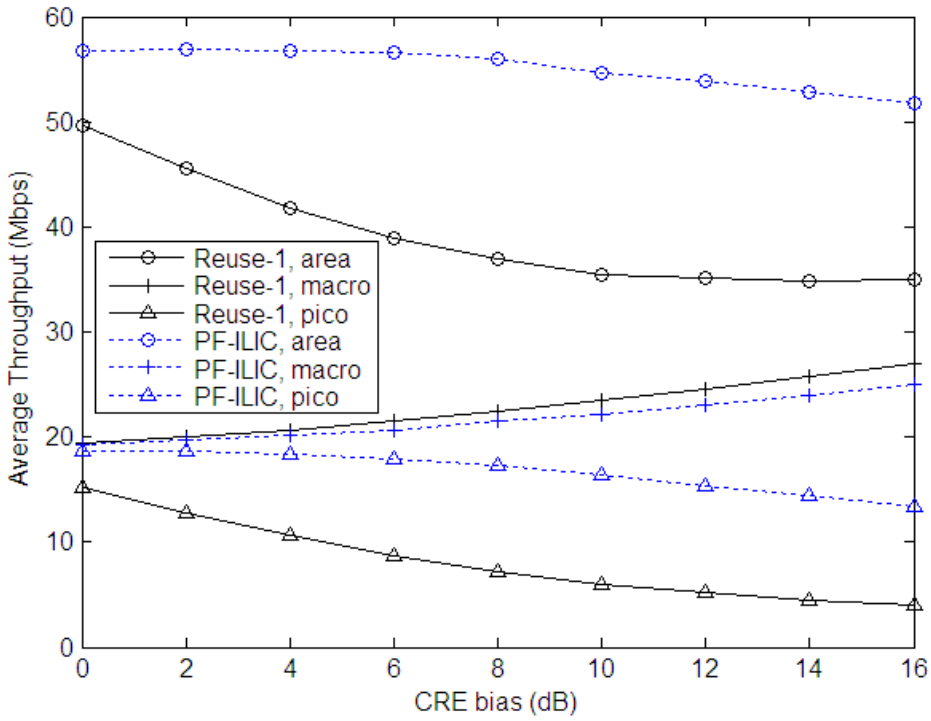

Fig. 4-8 Average throughput performance with different CRE bias values

4.5.4 Consideration on Fairness

As mentioned earlier, one of the important requirements for designing 4G systems is to have a more uniform user data rate experience among UEs across cells. Here, to this end, we bring in a parameter $\hat{f}$, called *layer fairness index*, to represent the data-rate fairness between macro-layer and pico-layer, and it is defined as

$$\hat{f} = \frac{T_{Cell}^{pico} / N_u^{pico}}{T_{Cell}^{macro} / N_u^{macro}}, \tag{4-22}$$

where N_u^{macro} is the average number of users per macrocell while N_u^{pico} is the average number of users per picocell. In this work, we consider three fairness cases: the first one is $\hat{f} = 1$, which is called *fair*; the second case is $\hat{f} = 2$, which is called *less fair*; and the last one is $\hat{f} = 3$, which is called *least fair*. In others words, in the above three cases, the average user throughputs of MUEs are, respectively, 100%, 50%, and 33.3% of the average users throughputs of PUEs. According to our simulation results, the selected CRE bias values that can closely achieve *fair*, *less fair*, and *least fair* for the conventional reuse-1 scheme are 9.3 dB, 6.6 dB, and 5 dB, respectively, and the corresponding CRE bias values for the PF-ILIC scheme are 15.2 dB, 11.2 dB, and 8.8 dB, respectively.

The simulation results of the average macrocell area throughput in different fairness cases are presented in Fig. 4-9. For reference, the result of the case without CRE (i.e. bias=0dB) is also shown in the figure. From Fig. 4-9, it is observed that the PF-ILIC scheme outperforms the reuse-1 scheme by about 45%, 42%, and 37% in macrocell area throughput in the *fair*, *less fair*, and *least fair* cases, respectively. This suggests that the PF-ILIC scheme is an effective method to achieve data-rate fairness between macro-layer

and pico-layer while maintaining satisfactory total system capacity. In addition, we notice that the system without CRE can yield good enough macrocell area throughput, but suffers from fairness problems since the average user throughput of PUEs is more than 10-fold higher ($\hat{f} \approx 10.6$) than that of MUEs.

Another meaningful metric to examine is the aggregated cell-edge throughput (T_{Edge}^{area}), which represents the total capacity of cell-edge users per single-macrocell coverage area and can be written as

$$T_{Edge}^{area} = T_{Edge}^{macro} + N_p \cdot T_{Edge}^{pico}. \quad (4\text{-}23)$$

Figure 4-10 demonstrates the average aggregated cell-edge throughput vs. layer fairness performance and the result in the case without CRE is also plotted as a reference. As shown in the figure, the PF-ILIC scheme is better than the reuse-1 scheme by approximately 91%, 42%, and 14% in aggregated cell-edge throughput in the *fair*, *less fair*, and *least fair* cases, respectively. This can be understood since the degraded throughput for the HetNet with reuse-1 scheme comes with the fast increase of service outage users. Combining the findings from Fig. 4-9 and Fig. 4-10, we conclude that as compared with the conventional reuse-1 scheme, the PF-ILIC scheme leads to substantially improvements in terms of overall system throughput as well as cell-edge throughput when considering a given layer fairness index; and further, the performance benefits are more pronounced when more fairness across different layers is required.

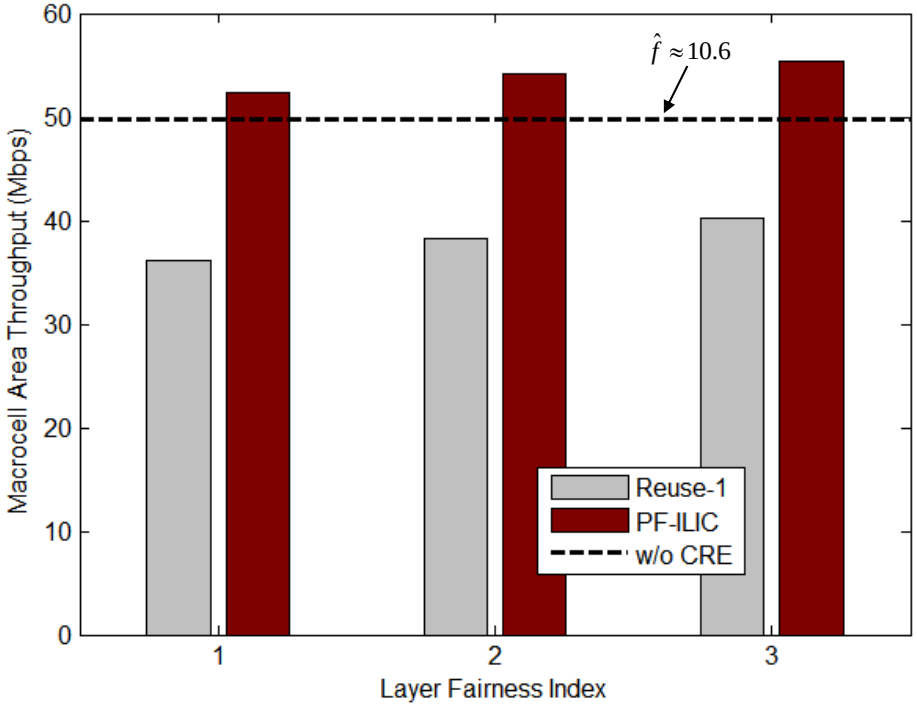

Fig. 4-9 Macrocell area throughput performance under different layer fairness criteria

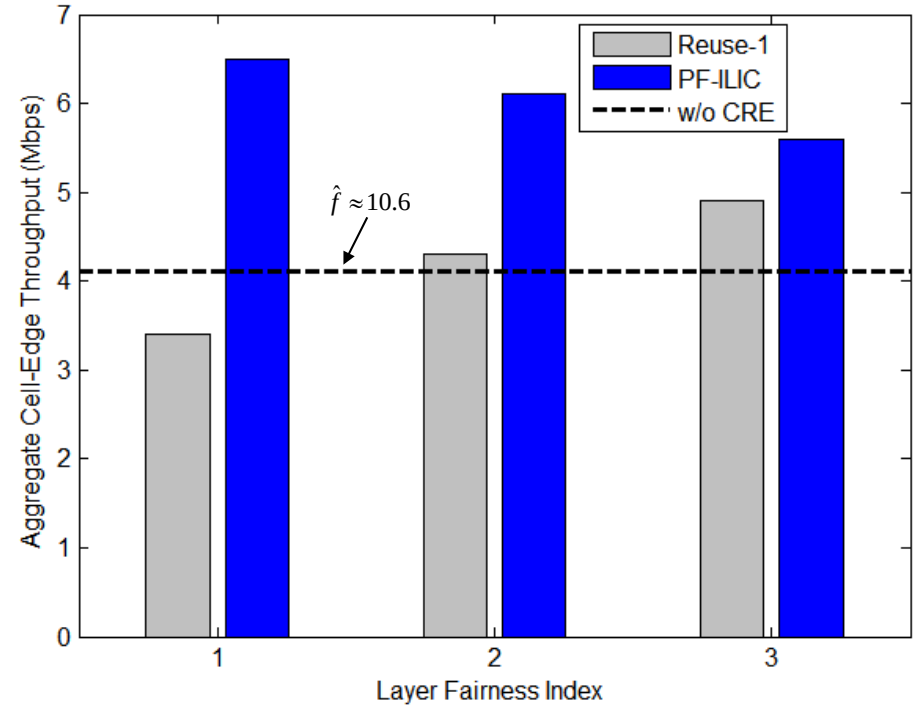

Fig. 4-10 Aggregated cell-edge throughput performance under different layer fairness criteria

4.6 Summary

Through deploying additional low-power nodes (LPNs) under the coverage area of a macrocell, heterogeneous network (HetNet) or multi-layered network deployments could be critical for operators to boost system capacity (per unit area) and support higher user data rate. In order to extent the coverage region of open access LPNs and hence offload more traffics from macrocells, cell range expansion (CRE) strategy is suggested to apply in HetNets. However, when macrocells and LPNs share the same spectrum, the total network throughput could actually decrease due to range expansion if the inter-layer interference couldn't be effectively managed.

In this chapter, we present a downlink inter-layer interference coordination scheme for an OFDMA co-channel macro-pico HetNet where the CRE technique is used. The proposed scheme can be seen as a joint power and frequency coordination technique accompanied with a set of resource allocation rules. For comparisons, the evaluations are conducted for the system with the proposed scheme and that with the conventional reuse-1 scheme. Our simulation results demonstrate that as compared with the reuse-1 scheme, the proposed scheme can lead to a significant improvement in link quality for those users in the extended region, and thereby greatly reduce the outage rate in the system. Moreover, even if there is a small loss in macrocell throughput, our approach provides a substantial total area throughput gain over the reuse-1 scheme. Considering data-rate fairness across layers (i.e. macro-layer and pico-layer), the proposed method outperforms the reuse-1 scheme in both total network throughput as well as cell-edge throughput. Overall, we conclude that the proposed scheme is an effective method to enhance system capacity and mitigate user outage in co-channel macro-pico HetNets that implement the picocell range expansion technique.

Chapter 5 Conclusions

IMT Advanced incorporates two 4G standards, they are 3GPP LTE-Advanced (also known as LTE Release 10), which is the evolved version of LTE, and WiMAX 2.0 (based on IEEE 802.16m), which is upgraded from Mobile WiMAX (based on IEEE 802.16e). These two emerging 4G standards both employ OFDMA as the downlink transmission scheme. However, in an OFDMA downlink system, as adjacent cells use the same frequency, inter-cell interference (ICI) may degrade the bit rate at cell edge. Inter-cell interference coordination (ICIC) is considered as a promising technology for alleviating this ICI and thus improving the cell edge data rate. In sum, ICIC is aimed to provide a more homogeneous throughput to users located in different regions of the network.

In this dissertation, we have studied ICI mitigation schemes in OFDMA systems and especially, we concentrate on the downlink side. The scope of our research encompasses ICIC schemes in cellular homogeneous networks as well as inter-layer interference coordination (ILIC) schemes in cellular heterogeneous networks (HetNets). It is worth noting that ILIC is also a kind of ICIC. There are three main contributions in our works.

Firstly, the performance of two widely accepted ICIC schemes, namely partial frequency reuse (PFR) and soft frequency reuse (SFR), have been evaluated and compared based on the signal strength difference based (SSD-based) user classification method, which is adopted in the LTE standard. Compared with the universal frequency reuse system, our simulation results show that both PFR and SFR schemes provide a significant cell edge throughput gain; however, a loss in total cell throughput usually comes up. Furthermore, based on a well defined data-rate fairness criterion, we show that PFR achieves a higher system capacity when compared to SFR. The second contribution is to present a hybrid ICI mitigation scheme, which makes use of both PFR and soft handover. The basic idea of this hybrid scheme is to dynamically select between a PFR scheme and a soft handover scheme to provide better signal quality for cell edge users. Compared with the standard PFR scheme, computer simulations show that approximately one quarter of cell edge users can get improvements in signal quality as well as link spectral efficiency from using the proposed hybrid scheme. We also observe that by using our approach, there is a significant cell edge throughput gain over the standard PFR scheme. Furthermore, considering the data rate fairness among users, we show that our method achieves higher overall system capacity as compared with the standard partial frequency reuse scheme. The final contribution of this dissertation is the development of an ILIC scheme that enables to deal with inter-layer interference in a co-channel macro-pico HetNet that carrying out (pico)cell range expansion (CRE) technique. The idea of the proposed method is to coordinate frequency and power resources among macrocells and picocells with a set of resource allocation rules. Simulation results show that the proposed method can bring a significant increase in overall system capacity as well as reduce the user outage rate in the system, especially when aggressive CRE is applied.

Next generation mobile communication systems make mobile broadband a reality,

improving transmission bit rate at cell edges will become a pressing problem. In the short term for cellular homogeneous deployments, ICIC strategies could serve to achieve more uniform user experience while maintain acceptable system capacity. It is worthy to note that *static* ICIC schemes are attractive for operators since the complexity of their deployment is very low. In the long term, a combination of ICIC/ILIC and CoMP could potentially employ to further enhance the system performance not only for cellular homogeneous networks, but also for cellular HetNets. However, while ICIC techniques are primary designed for static or semi-static operation, CoMP techniques target more dynamic coordination [17]. As a result, the backhaul requirements, both in terms of throughput and latency become the top challenge issue for CoMP implementation. Note that the exact requirements depend on different downlink CoMP technologies being considered (e.g., CS/CB, DCS or JT). In addition, excessive (uplink) feedback overhead introduced by CoMP could also be a problem. Therefore, there will be a subject of designing effective CoMP or hybrid CoMP/ICIC schemes that take practical limitations as well as uplink overhead into account for future research.

References

[1] Cisco, “Cisco Visual Networking Index: Global Mobile Data Traffic Forecast Update, 2011-2016,” *Cisco White Paper*, Feb. 2012.

[2] IEEE 802.16e-2005, “Part 16: Air Interface for Fixed Broadband Wireless Access Systems, Amendment for physical and MAC layers for combined fixed and mobile operation in licensed bands,” 2005.

[3] Recommendation ITU-R M.1645, “Framework and Overall Objectives of the Future Development of IMT-2000 and Systems Beyond IMT-2000,” *ITU-R Radio Assembly*, June 2003.

[4] IEEE 802.16m-2011, “IEEE Standard for Local and Metropolitan Area Networks Part 16: Air Interface for Broadband Wireless Access Systems Amendment 3: Advanced Air Interface,” May 2011.

[5] 3GPP TS 36.201 V8.3.0, “Evolved Universal Terrestrial Radio Access (E-UTRA); LTE Physical Layer - General Description,” Mar. 2009.

[6] 3GPP TR 25.913 V7.0.0, “Requirements for Evolved UTRA (E-UTRA) and Evolved UTRAN (E-UTRAN),” June 2005.

[7] 3GPP TR 25.913 V7.0.0, “Requirements for Evolved UTRA (E-UTRA) and Evolved UTRAN (E-UTRAN),” June 2005.

[8] 3GPP TR 36.913 V8.0.1, “Requirements for further advancements for Evolved Universal Terrestrial Radio Access (E-UTRA),” Mar. 2009.

[9] Siemens, “Interference mitigation – Considerations and Results on Frequency Reuse,” 3GPP R1-050738, *3GPP TSG RAN WG1 Meeting #42*, September 2005.

[10] M. Sternad, T. Ottosson, A. Ahlen, A. Svensson, “Attaining both coverage and high spectral efficiency with adaptive OFDM downlinks,” in Proc. *IEEE 58th Veh. Technol. Conf.*, vol. 4, pp. 2486-2490, Oct. 2003.

[11] Huawei, “Soft Frequency Reuse Scheme for UTRAN LTE,” 3GPP R1-050507, *3GPP TSG RAN WG1 Meeting #41*, May 2005.

[12] Bin Fan, Yu Qian, Kan Zheng, Wenbo Wang, “A Dynamic Resource Allocation Scheme Based on Soft Frequency Reuse for OFDMA Systems,” in Proc. *Int. Symp. Microwave, Antenna, Propagation and EMT Tech. for Wireless Commu.*, pp. 1-4, Aug.

2007.

[13] Alcatel, “Interference Coordination in new OFDM DL air interface,” 3GPP R1-050407, *3GPP TSG RAN WG1 Meeting #41*, May 2005.

[14] Harri Holma and Antti Toskala, *LTE for UMTS – OFDMA and SC-FDMA Based Radio Access*, John Wiley & Sons, 2009.

[15] 3GPP TR 36.814 V9.0.0, “Further advancements for E-UTRA physical layer aspects,” Mar. 2010.

[16] 3GPP TR 36.819 V11.0.0, “Coordinated multi-point operation for LTE physical layer aspects,” Dec. 2011.

[17] Daewon Lee, Hanbyul Seo, Bruno Clerckx, Eric Hardouin, David Mazzarese, Satoshi Nagata, Krishna Sayana, “Coordinated Multipoint Transmission and Reception in LTE-Advanced: Deployment Scenarios and Operational Challenges,” *IEEE Commun. Mag.*, vol. 50, no. 2, pp. 148-155, Feb. 2012.

[18] Xu Xiaodong, Chen Xin, Li Jingya, “Handover Mechanism in Coordinated Multi-Point Transmission/Reception System,” *ZTE Communications*, no. 1, pp. 31-35, Mar. 2010.

[19] D. Astély, E. Dahlman, A. Furuskär, Y. Jading, M. Lindström, and S. Parkvall, “LTE: the evolution of mobile broadband,” *IEEE Commun. Mag.*, vol. 47, no. 4, pp. 44-51, April 2009.

[20] CMCC, “New Work Item Proposal: Enhanced ICIC for non-CA based deployments of heterogeneous networks for LTE,” 3GPP RP-100383, *3GPP TSG RAN Meeting #47*, Mar. 2010.

[21] A. Damnjanovic, J. Montojo, Y. Wei, T. Ji, T. Luo, M. Vajapeyam, T. Yoo, O. Song, and D. Malladi, “A survey on 3GPP heterogeneous networks,” *IEEE Wireless Commun.*, vol. 18, no. 3, pp. 10–21, June 2011.

[22] Lopez-Perez and X. Chu, “Inter-cell interference coordination for expanded region picocells in heterogeneous networks,” in Proc. *IEEE Int. Conf. Computer Commun. Networks (ICCCN)*, pp. 1-6, Aug. 2011.

[23] Qualcomm, “Importance of Serving Cell Selection in Heterogeneous Networks,” 3GPP R1-100701, *3GPP TSG RAN WG1 Meeting #59*, Jan. 2010.

[24] A. Khandekar, N. Bhushan, Ji Tingfang, and V. Vanghi, “LTE-Advanced: Heterogeneous networks,” in Proc. *2010 European Wireless Conference*, pp. 978-982,

April 2010.

[25] Lopez-Perez, D. Guvenc, I. de la Roche, G. Kountouris, M. Quek, T.Q.S., Jie Zhang, "Enhanced intercell interference coordination challenges in heterogeneous networks," *IEEE Wireless Commun.*, vol. 18, no. 3, pp. 22-30, June 2011.

[26] Texas Instruments, "Performance of Inter-Cell Interference Mitigation with Semi-Static Frequency Planning for EUTRA Downlink," 3GPP R1-060368, *3GPP TSG RAN WG1 Meeting #44*, Feb. 2006.

[27] Ericsson, "Downlink Inter-Cell Interference Co-ordination/Avoidance – Evaluation of Frequency Reuse," 3GPP R1-061374, *3GPP TSG RAN WG1 Meeting #45*, May 2006.

[28] Yikang Xiang, Jijun Luo, C. Gorg, "Performance Impact of User Grouping on Fractional Power Loading in the OFDMA Downlink," in Proc. *IEEE Symp. 18th PIMRC*, Sep. 2007.

[29] M. Rahman, H. Yanikomeroglu, W. Wong, "Interference Avoidance with Dynamic Inter-Cell Coordination for Downlink LTE System," in Proc. *IEEE WCNC'09*, Apr. 2009.

[30] Haipeng Lei, Zhang Lei, Xin Zhang, Dacheng Yang, "A Novel Multi-Cell OFDMA System Structure using Fractional Frequency Reuse," in Proc. *IEEE 18th PIMRC*, Sept. 2007

[31] 3GPP TSG RAN WG1, "LS on additional RSRP trigger for ICIC," 3GPP R1-083272, *3GPP TSG RAN WG1 Meeting #54*, Aug. 2008.

[32] Motorola, "CoMP Operation and Evaluation," 3GPP R1-091935, *3GPP TSG RAN WG1 Meeting #57*, May 2009.

[33] S.-E. Elayoubi, O. Ben Haddada, B. Fourestie, "Performance evaluation of frequency planning schemes in OFDMA-based networks," *IEEE Trans. on Wireless Communications*, vol. 7, no. 5, pp. 1623-1633, May 2008..

[34] R. Y. Chang, Zhifeng Tao, Jinyun Zhang, C.-C.J. Kuo, "A Graph Approach to Dynamic Fractional Frequency Reuse (FFR) in Multi-Cell OFDMA Networks," in Proc. *IEEE Int. Conf. Commun. (ICC'09)*, June 2009.

[35] K. Doppler, C. Wijting, K. Valkealahti, "Interference Aware Scheduling for Soft Frequency Reuse," in Proc. *IEEE 69th Veh. Technol. Conf.*, April 2009.

[36] Farooq Khan, *LTE for 4G Mobile Broadband: Air Interface Technologies and Performance*, Cambridge, 2009.

[37] Siemens, “Interference Mitigation by Partial Frequency Reuse,” 3GPP R1-060135, *3GPP TSG RAN WG1 Ad Hoc Meeting on LTE*, Jan. 2006.

[38] Stefania Sesia, Issam Toufik, Matthew Baker, *LTE - The UMTS Long Term Evolution: From Theory to Practice*, John Wiley, Sept. 2011.

[39] H. Jia, Z. Zhang, G. Yu, P. Cheng, S. Li, “On the Performance of IEEE 802.16 OFDMA System Under Different Frequency Reuse and Subcarrier Permutation Patterns”, in Proc. *IEEE Int. Conf. Commun.*, pp. 5720-5725, June 2007,

[40] Texas Instruments, “Inter-Cell Interference Mitigation for EUTRA”, 3GPP R1-051059, *3GPP TSG RAN WG1 Meeting #42bis*, October 2005.

[41] Shannon, C.E., “Collected Papers,” Edit by Sloane & Wyner, IEEE Press, 1993.

[42] P. Mogensen, Wei Na, I.Z. Kovacs, F. Frederiksen, A. Pokhariyal, K.I. Pedersen, T. Kolding, K. Hugl, M. Kuusela, “LTE Capacity Compared to the Shannon Bound,” in Proc. *IEEE 65th Veh. Technol. Conf.*, pp. 1234-1238, April 2007.

[43] Qualcomm Europe, “Description and simulations of interference management technique for OFDMA based E-UTRA downlink evaluation,” 3GPP R1-050896, *3GPP TSG RAN WG1 Meeting #42*, Sept. 2005.

[44] 3GPP TR 25.814 v7.1.0, “Physical Layer Aspects for Evolved UTRA”, Sept. 2006.

[45] Orange, China Mobile, KPN, NTT DoCoMo, Sprint, T-Mobile, Vodafone, Telecom Italia, “Inter-Cell Interference Mitigation for EUTRA”, 3GPP R1-070674, *3GPP TSG RAN WG1 Meeting #48*, Feb. 2007.

[46] Huawei, “Power Allocation among eNBs in Close-Loop Downlink CoMP Transmission with CA”, 3GPP R1-091268, *3GPP TSG RAN WG1 Meeting #56bis*, Mar. 2009.

[47] NTT DoCoMo, “Investigation on Coordinated Multipoint Transmission Schemes in LTE-Advanced Downlink,” 3GPP R1-090314, *3GPP TSG RAN WG1 Meeting #55bis*, Jan. 2009.

[48] A.J. Viterbi, AM. Viterbi, KS. Gihousen, E. Zehavi, “Soft handoff extends CDMA cell coverage and increase reverse link capacity,” *IEEE J. Sel. Areas Commun.*, vol. 12, pp. 1281-1288, Oct. 1994.

[49] H. Holma and A. Toskala, *WCDMA for UMTS*, 3rd edition, Wiley, 2002.

[50] Renshui Zhu, Xing Zhang, Wenbo Wang, “Scheduling Based Controllable

Interference Coordination in OFDMA Systems," in Proc. *First Internation Conference on Communications and Networking*, pp. 1-5, Oct. 2006.

[51] NTT DoCoMo, NEC, SHARP, "Intra-Node B Macro Diversity Using Simultaneous Transmission with Soft-combining in Evolved UTRA Downlink", 3GPP R1-050700, *3GPP TSG RAN WG1 Meeting #42*, September 2005

[52] Jian Huang, P. Xiao, Xiaojun Jing, "A downlink ICIC method based on region in the LTE-Advanced system," *2010 IEEE PIMRC Workshops*, pp. 420-423, Sept. 2010.

[53] ASB, Alcatel-Lucent, "DL Pico/Macro HetNet Performance: Cell Selection," 3GPP R1-101873, *3GPP TSG RAN WG1 Meeting #60bis*, April 2010.

[54] Tongwei Qu, Dengkun Xiao, Dongkai Yang, Wei Jin, Yuan He, "Cell selection analysis in outdoor heterogeneous networks," in Proc. *2010 IEEE ICACTE*, pp. V5-554 – V5-557, Aug. 2010.

[55] Alcatel, "Comparison of efficiency of DL Interference Coordination schemes and view on measurements on intra-frequency neighbor cells," 3GPP R1-062365, *3GPP TSG RAN WG1 Meeting #46*, Aug. 2006.

[56] Alcatel-Lucent Shanghai Bell, Alcatel-Lucent, "Interference analysis for Type I and Type II Relay," 3GPP R1-092154, *3GPP TSG RAN WG1 Meeting #57*, May 2009.

[57] Samsung, "Cell Range Expansion Performance Evaluation," 3GPP R1-105408, *3GPP TSG RAN WG1 Meeting #62bis*, Oct. 2010.

[58] 3GPP TR 36.942 V8.3.0, "E-UTRA Radio Frequency (RF) System Scenarios," Sept. 2010.

[59] Nokia Siemens Networks, Nokia, "Initial Results and Assumptions for LTE-Advanced Heterogeneous Scenarios," 3GPP R1-093329, *3GPP TSG RAN WG1 Meeting #58*, Aug. 2009.

[60] Nokia Siemens Networks, Nokia, "Downlink CCH performance aspects for co-channel deployed macro and HeNBs," 3GPP R1-100350, *3GPP TSG RAN WG1 Meeting #59bis*, Jan. 2010.

Vita

Che-Sheng Chiu was born in Chiayi, Taiwan, R.O.C., in 1975. He received his B.S. degree in Applied Mathematics from National Chiao Tung University, Hsinchu, Taiwan, in 1997. He pursued his M.S. and Ph.D. in the Department of Communication Engineering under the supervision of Professor Chia-Chi Huang in National Chiao Tung University, and was graduated in 1999 and 2012, respectively.

Since 2000, he has been with Telecommunication Laboratories, Chunghwa Telecom Company, working on 3GPP LTE and LTE-Advanced standardization. His research interests include radio network resource management, mobile network system-level performance evaluation, and cross-layer optimization for high-speed wireless networks.

Author's Publications (2006~2012)

A. Journal Papers

1. C.-S. Chiu and C.-C. Huang, "Performance Comparison between Two Inter-Cell Interference Coordination Schemes for OFDMA Downlink Systems," *International Journal of Electrical Engineering*, vol. 18, no. 1, pp. 19-26, Feb. 2011.
2. C.-S. Chiu and C.-C. Huang, "A Hybrid Inter-Cell Interference Mitigation Scheme for an OFDMA Downlink System," *IEICE Transaction on Communications*, vol. E93-B, no. 1, pp. 73-81, Jan. 2010.

B. Conference Papers

3. C.-S. Chiu and C.-C. Huang, "An Interference Coordination Scheme for Picocell Range Expansion in Heterogeneous Networks", in *Proc. IEEE Vehicular Technology Conference 2012 (VTC2012-Spring)*, May 2012.
4. C.-S. Chiu and C.-C. Huang, "Combined Partial Reuse and Soft Handover in OFDMA Downlink Transmission", in *Proc. IEEE Vehicular Technology Conference 2008 (VTC2008-Spring)*, May 2008.
5. C.-S. Chiu and C.-C. Huang, "Improving Inter-Sector Handover User Throughput by Using Partial Reuse and Softer Handover in 3GPP LTE Downlink", in *Proc. The 14th International Conference on Advanced Communication Technology (ICACT2008)*, Feb. 2008.
6. C.-S. Chiu and C.-C. Huang, "A Study on Fast Sector Selection with Frequency Coordination in E-UTRA Downlink," in *Proc. The 4th IEEE VTS Asia Pacific Wireless Communications Symposium*, Aug. 2007.
7. C.-S. Chiu and C.-C. Huang, "On Inter-Sector Macro Diversity for 3GPP LTE Downlink," in *Proc. 2006 National Symposium on Telecommunications*, Dec. 2006.